We would like to thank the reviewer for the evaluation of our study and the constructive comments that helped us to improve the manuscript. Please find below the reviewer's comments in black font and the author's response in blue font.

Responses to Anonymous Referee #1

- In the revised manuscript, we added one new subsection 3.1 to show the seasonal mean difference of T2M, total precipitation and snowfall over the pan-Arctic sea ice and added one new figure (Figure 2). Accordingly, the original section 3.1 changed to 3.2, and the original subsection 3.1 and 3.2 changed to 3.2.1 and 3.2.2, respectively.
- We replotted the original Figure 2 and 3 which named as Figure 3 and 4 in the revised manuscript,
  - In the new Figure 3 we show the variation of T2M from ERA5, ERA-I and buoys and the differences of T2M between ERA5 and ERA-I for 5 buoys, plots for the other buoys are provided in the Supplementary Information as Figure S1 and S2.
  - In the new Figure 4 we show the variation of T2M differences between ERA5/ERA-I and buoys for the same 5 buoys as in the new Figure 2. Plots for the other buoys are provided in the Supplementary Information as Figure S3.
- We added a new Figure 6 to show the T2M difference between ERA5/ERA-I and buoys in four regions (Central Arctic, Atlantic sector, Pacific sector, and Laptev Sea) in the Arctic. Correspondingly, we added one paragraph at the end of the original section of 3.1 to describe the regional differences.
- We replotted the original Figures 5 and 6, the new figure is now Figure 7 and Figure S4-5. In these new figures, we show the accumulated total precipitation and snowfall from ERA5 and ERA-I and snow depth measured by buoys.
- The original Figure 7 (showing the FDD and sea ice growth) was moved to Supplementary Information as Figure S6, and the discussion on the FDD model was shortened.
- Forcing data of wind speed (V), relative humidity (Rh) and total cloud (CN) and ocean heat flux were plotted and provided in the Supplementary Information as Figure S7.

Our specific responses are given below.

In the abstract, I would not say that ERA-I is drier than 'most' reanalyses, I will say ERA-I is drier than 'some' reanalyses - see Boisvert et al., 2018 Journal of Climate

Agree. Changed to "ERA-I is drier than some modern reanalyses".

Figure 3 caption. Do you mean panel (D), not (K)? Because there is no panel K in the figure.

Thank you for spotting this typo. In the revised manuscript, we have replotted Figure 3. We now show only five buoys, and moved the remaining buoys to Figures S1-2 in the Supplementary Information (see below) to keep the main text concise.

It would be great to see a little more conversation dealing with the differences in Temp and Precipitation compared to the buoys and to themselves. It seemed like some regions where the buoys were/times of the year produce larger differences between the buoys and the reanalyses. For example, there appeared to be larger differences between realanyses and the buoys in the Beaufort sea areas.

We now include a new Figure (Fig. 2), showing the regional and seasonal differences of Temp, total precipitation and snowfall over the pan-Arctic sea ice between ERA5 and ERA-I. These analyses are discussed in the new subsection 3.1. In addition, we have made a new figure (Figure 6), showing the Temp differences between buoys and the reanalyses for different regions, including: the Central Arctic (north of 86° N), Pacific sector (90° W – 150°E), Atlantic sector (30° W – 60° E) and Laptev Sea (60° E – 150° E). This reveals that the differences are large in the Atlantic sector and small in the Central Arctic. New Figure 2 and 6 are shown below. The subsection 3.1 reads as,

"3.1 Spatial distribution of seasonal difference of reanalysis near surface temperature and precipitation

Figure 2 shows the seasonal mean differences of T2M, total precipitation and snowfall between ERA5 and ERA-I over Arctic sea ice during 2010-2015. We classify spring as March, April and May, summer as June, July and August, autumn as September, October and November, and winter as December, January and February. The seasonal mean ice extent is obtained from the monthly sea ice concentration from NOAA/NSIDC during 2010-2015 (Meier et al., 2017).

The difference in T2M between ERA5 and ERA-I clearly varies with season (Fig. 2a-d). ERA5 is generally warner than ERA-I in spring and winter, and colder than ERA-I during summer and autumn over most regions of Arctic sea ice. These temperature differences are small during summer, but large during the other seasons. Near the North Pole, ERA5 is warmer than ERA-I in summer, but colder than ERA-I in winter. Whether warmer or colder, the differences between ERA5 and ERA-I are small (<±0.4 °C) in this region.

ERA-I is known to be a relatively "dry" global reanalysis product in the Arctic compared with most other modern reanalyses (e.g. MERRA-2, CFSR, and JRA-55) (Lindsay et al., 2014; Merkouriadi et al., 2017; Boisvert et al., 2018). However, the total precipitation in ERA5 is lower than in EAR-I over Arctic sea ice in all seasons (Fig. 2e-h). The lower precipitation in ERA5 is most pronounced in summer, and in the eastern Arctic. Differences in the snowfall between ERA5 and ERA-I are smaller than for total precipitation (Fig. 2 i-j vs. Fig. 2e-h). The snowfall in ERA5 is lower than in ERA-I in spring, autumn and winter, but larger than ERA-I in summer.”

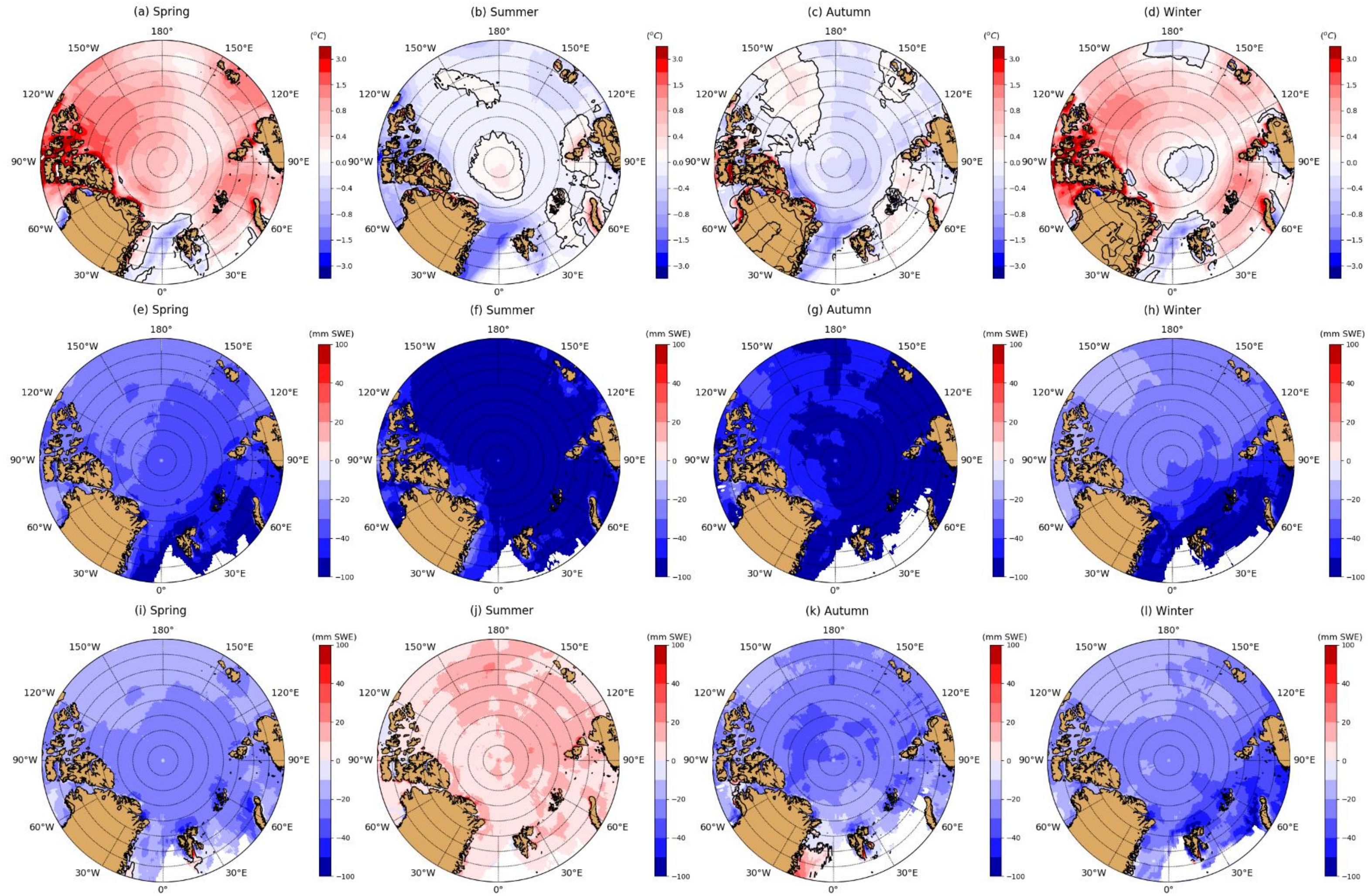

Figure 2. Seasonal mean difference between ERA5 and ERA-I (ERA5-ERA-I) for T2M (a-d), total precipitation (e-h), and snowfall (i-l) in spring (a, e, i), summer (b, f, j), autumn (c, g, k) and winter (d, h, l) over Arctic sea ice during 2010-2015. The mean sea ice extent in the seasonal is used for classification of sea ice and open ocean.

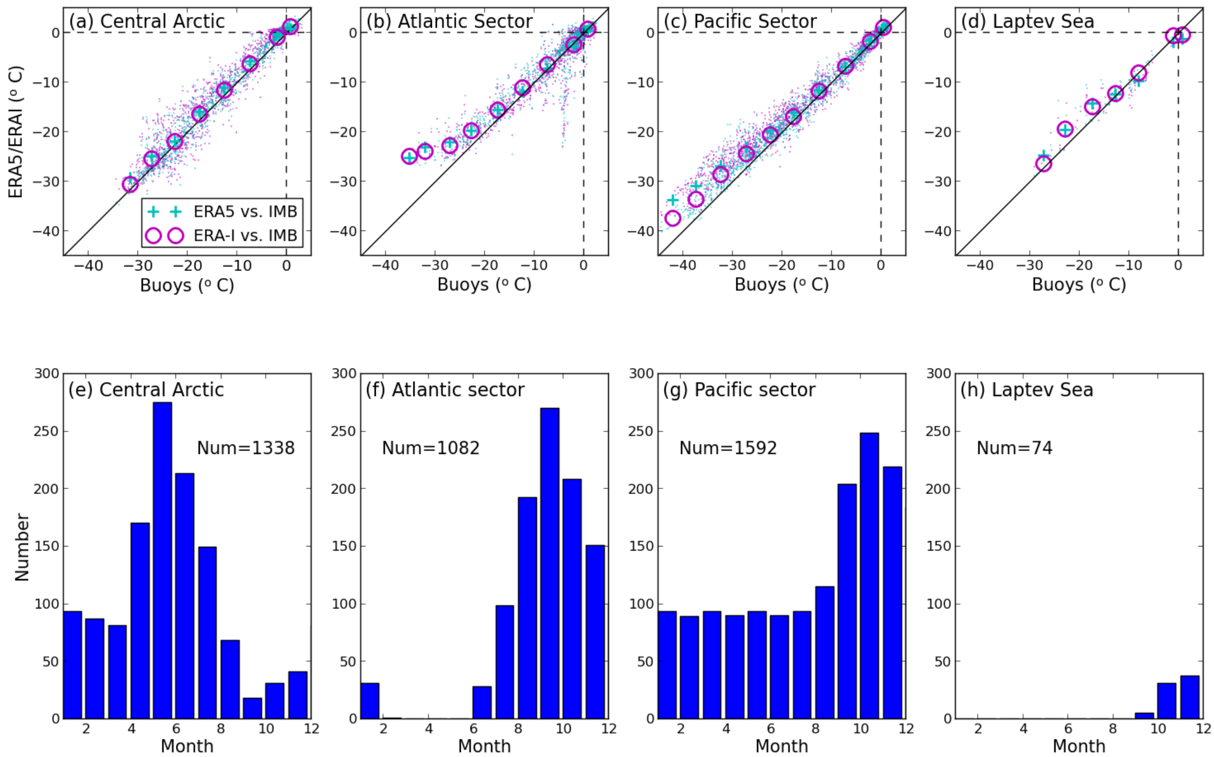

Figure 6. Scatter plot of T2M from ERA5 and ERA-I vs. from buoys in (a) Central Arctic, (b) Atlantic sector, (c) Pacific sector, and (d) Laptev Sea, and number of data (daily) in (e) Central Arctic, (f) Atlantic sector, (g) Pacific sector, and (h) Laptev Sea.

The text for describing Figure 6 read as follows "The performance of reanalysis near surface temperature varies with region over Arctic sea ice (Fig. 6, also refer to Fig. 2). According to the buoys' positions (Fig. 1), we define four regions in the Arctic: the Central Arctic (north of 86 °N), and the Pacific sector (90 °W – 150 °E), the Atlantic sector (30 °W – 60 °E), and the Laptev Sea (60 °E – 150 °E). The later three sectors are south of 86 °N. The ERA5/ERA-I near surface temperature performs best in the Central Arctic (Fig. 6a), and well in the Pacific sector (Fig. 6c). It performs well in the Atlantic sector when the T2M is above -25 °C, but poorly when the T2M is below -25 °C (Fig. 6b). The performance of reanalysis near surface temperature in the Laptev Sea needs to be further investigated due to small number of observations in this region (Fig. 6d & 6h). However, there is also some seasonal bias in the availability of data from buoys in the different regions, largely due to when buoys are deployed in different regions of the Arctic and ice drift patterns." Please also refer to P6 L25-33.

Figures 2 and 3. It would be beneficial to also have the differences between ERA5 and ERA-I and the buoy temperatures perhaps in a different figure? Because it is a little hard to see how well the reanalyses compare with the buoys the way it is now. Or perhaps provide a table with the differences and biases for each buoy.

To show the differences clearly, we replotted Figures 2 and 3 (see below). These are now Figures 3 and 4 in the revised manuscript.

In the new Figure 3, we show the variation of 2 m air temperature in ERA5, ERA-I and the buoys in a subplot, and the differences of T2M between ERA5 and ERA-I in a separate subplot below. Overall, there are five buoys shown in the new Figure 3. All the other buoys were shown as supplementary Figure S1 and S2.

In the new Figure 4, we show the differences between ERA5/ERA-I and the buoy measurements for five buoys as in Figure 3. The other buoys are shown in supplementary Figure S3.

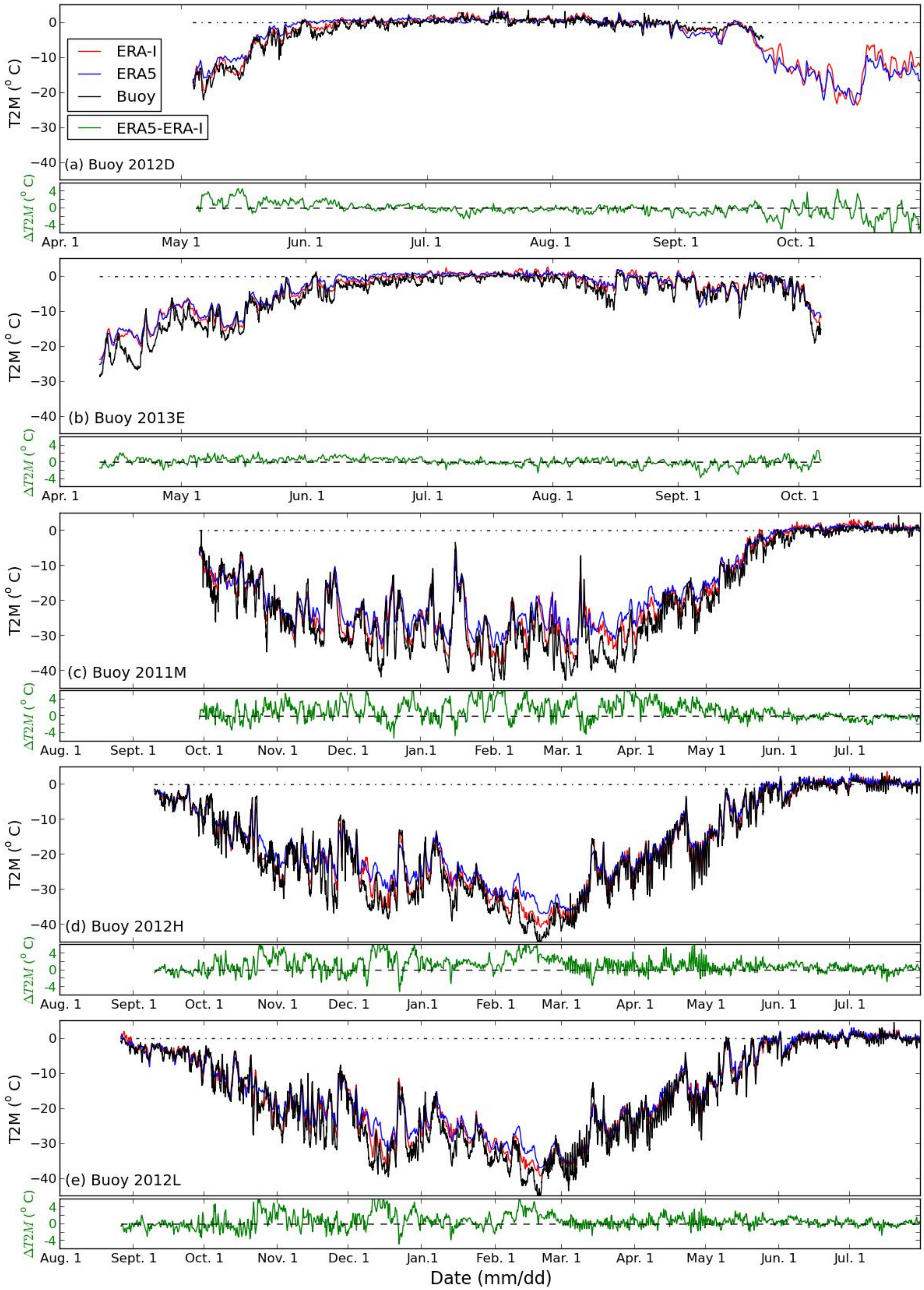

Figure 3. Variation of 2 m air temperature (T2M) in ERA5, ERA-I and the buoys and the difference of T2M between ERA5 and ERA-I for buoys (a) 2012D, (b) 2013E, (c) 2011M, (d) 2012H, and (e) 2012L. Note the different time-axes.

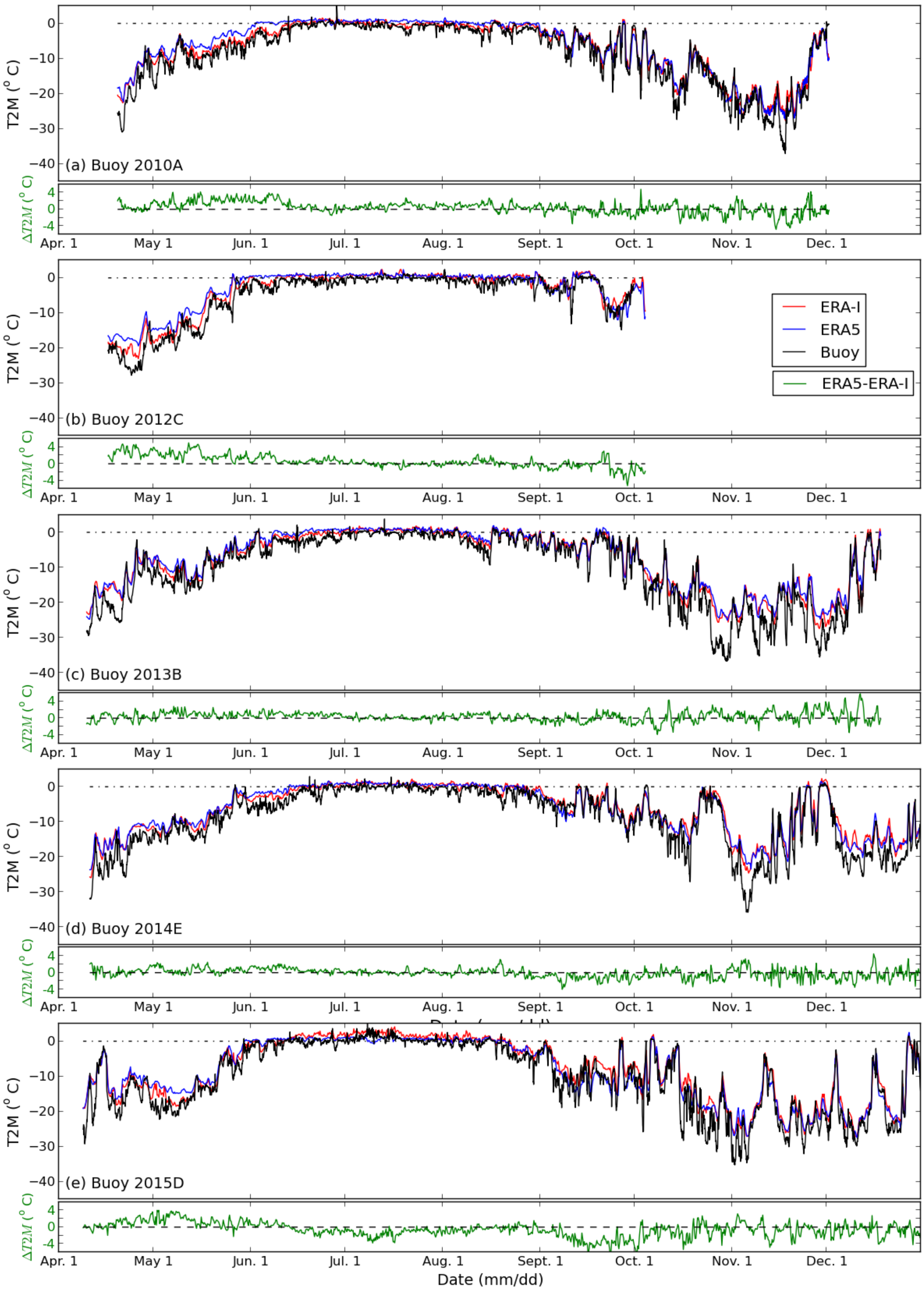

Figure S1. Variation of 2 m air temperature (T2M) in ERA5, ERA-I and the buoys and the difference of T2M between ERA5 and ERA-I for buoys (a) 2010A, (b) 2012C, (c) 2013B, (d) 2014E, and (e) 2015D.

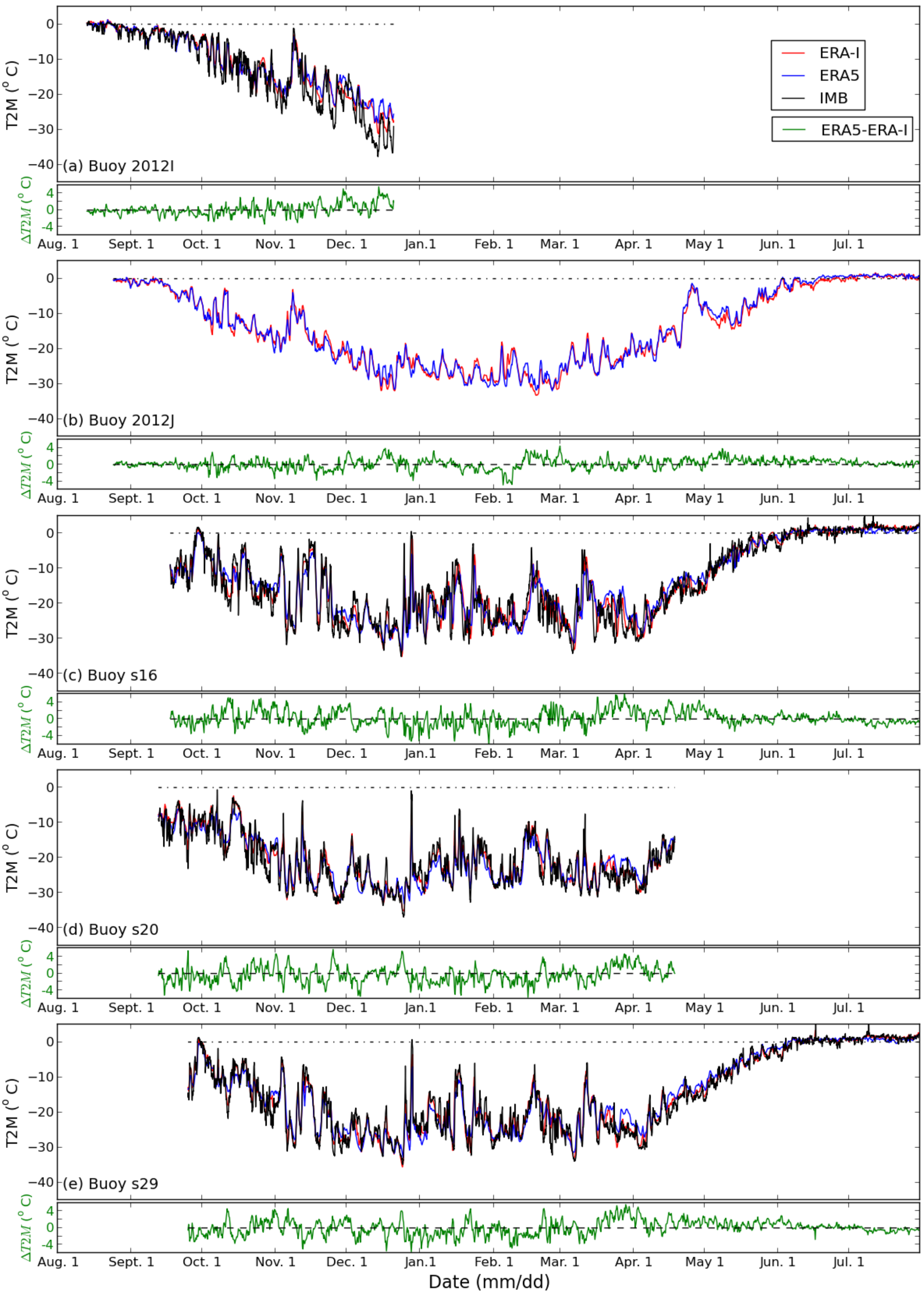

Figure S2. Same as Figure S1, but for buoys (a) 2012I, (b) 2012J, (c) s16, (d) s20, and (e) s29. Note there is no buoy data in Figure (b) for buoy 2012J.

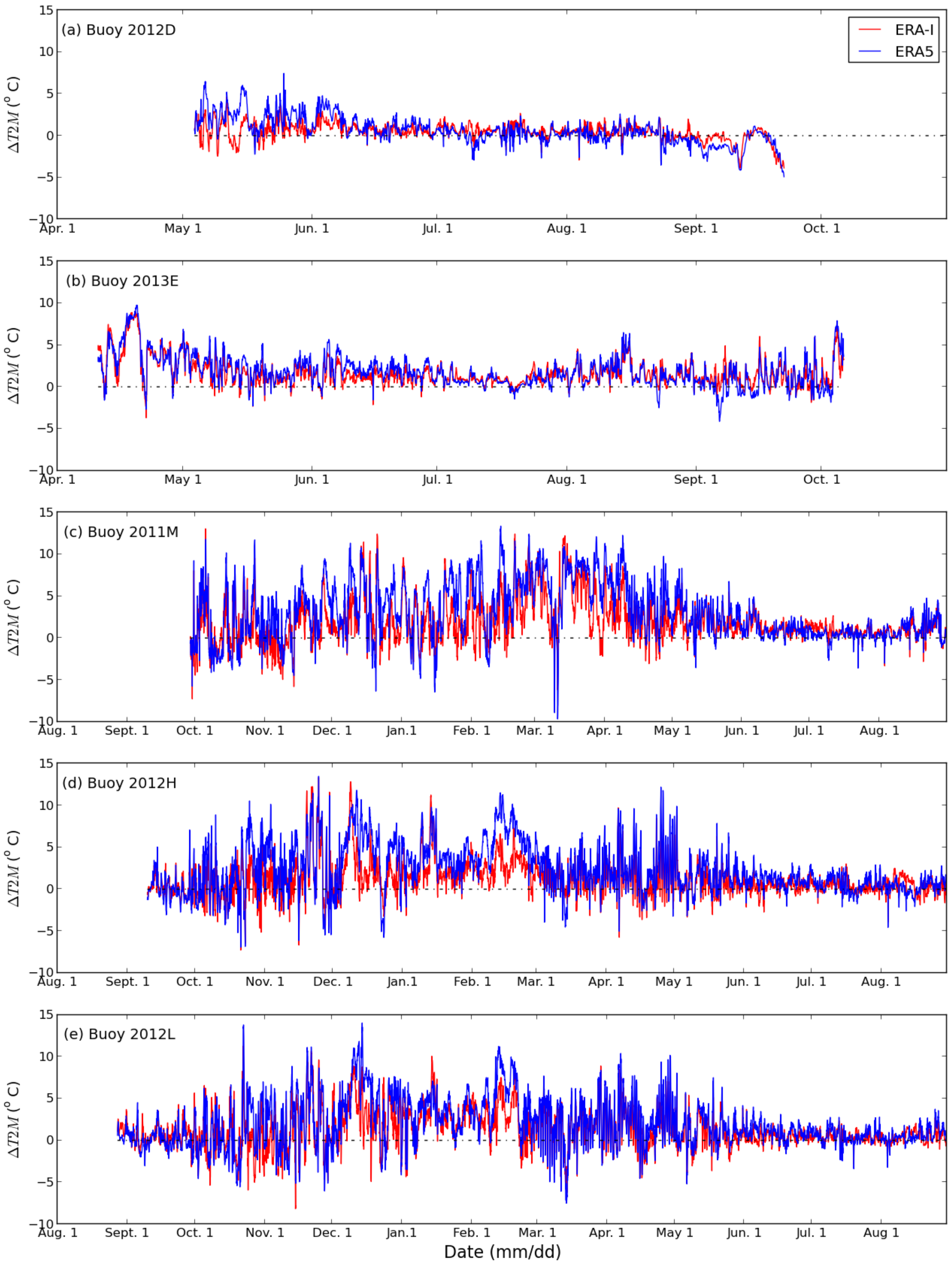

Figure 4. Variation of T2M differences between ERA5/ERA-I and buoys for (a) buoy 2012D, (b) buoy 2013E, (c) buoy 2011M, (d) buoy 2012H, and (e) buoy 2012L.

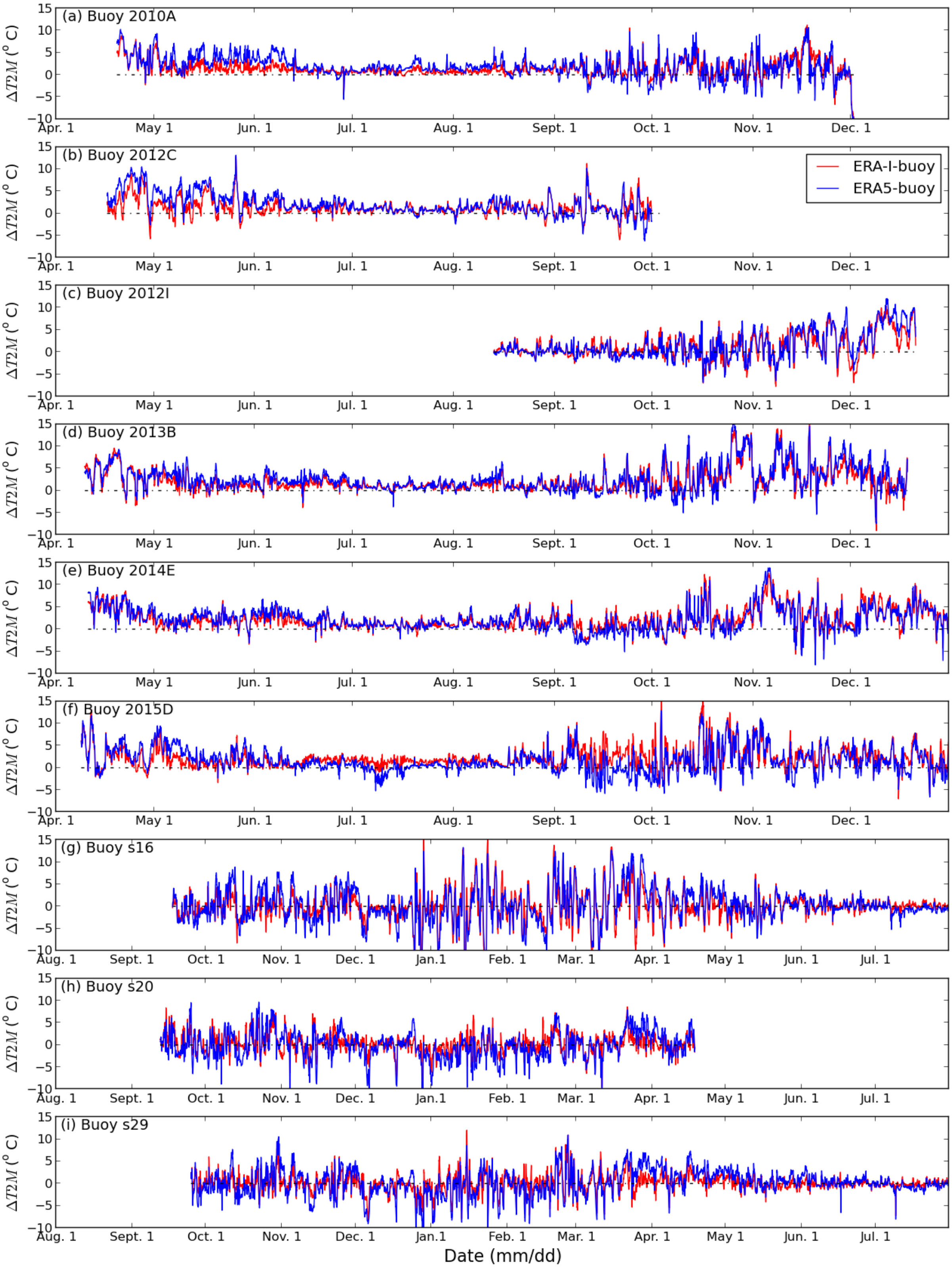

Figure S3. Variation of T2M differences between ERA5/ERA-I and buoys for (a) buoy 2010A, (b) buoy 2012C, (c) buoy 2012I, (d) buoy 2013B, (e) buoy 2014E, (f) buoy 2015D, (g) buoy s16, (h) buoy s20, and (i) buoy s29.

Page 4, line 16: Might be best to say where these 2 buoys are located in the text. 2013 E and 2012 J? Perhaps the reanalyses are better at producing accurate temperatures in certain regions of the Arctic and perhaps this could be elaborated on more.

Text of "which are both deployed in central Arctic, the former near the North Pole and the later closer to the Laptev Sea (Fig. 1)" was added to clarify where the 2 buoys were deployed (See P5 L22-23). To elaborate, we added a new figure (Figure 6) as mentioned above for T2M difference between buoys and the reanalyses in different regions: Central Arctic (north of 86° N), and south of 86° N we have the Pacific sector (90° W – 150°E), Atlantic sector (30° W – 60° E) and Laptev Sea (60° E – 150° E). Our new Figure 6 shows the reanalysis are best at producing accurate temperature in the Central Arctic.

I know that snow depths are fairly uncertain, but perhaps instead of taking a constant snow density of 350 kg/m3, why not time vary it throughout the winter season and based on locations based on the Warren climatology. This might improve your results.

Thanks for your suggestion. Instead of a constant snow density, a climatological monthly mean snow density was applied based on Fig. 11 of Warren et al. (1999). This results in the new Figure 7 and Figures S4 and S5, in which we show the precipitation/snowfall from reanalysis of ERA5 and ERA-I, and snow depth from buoys (see below).

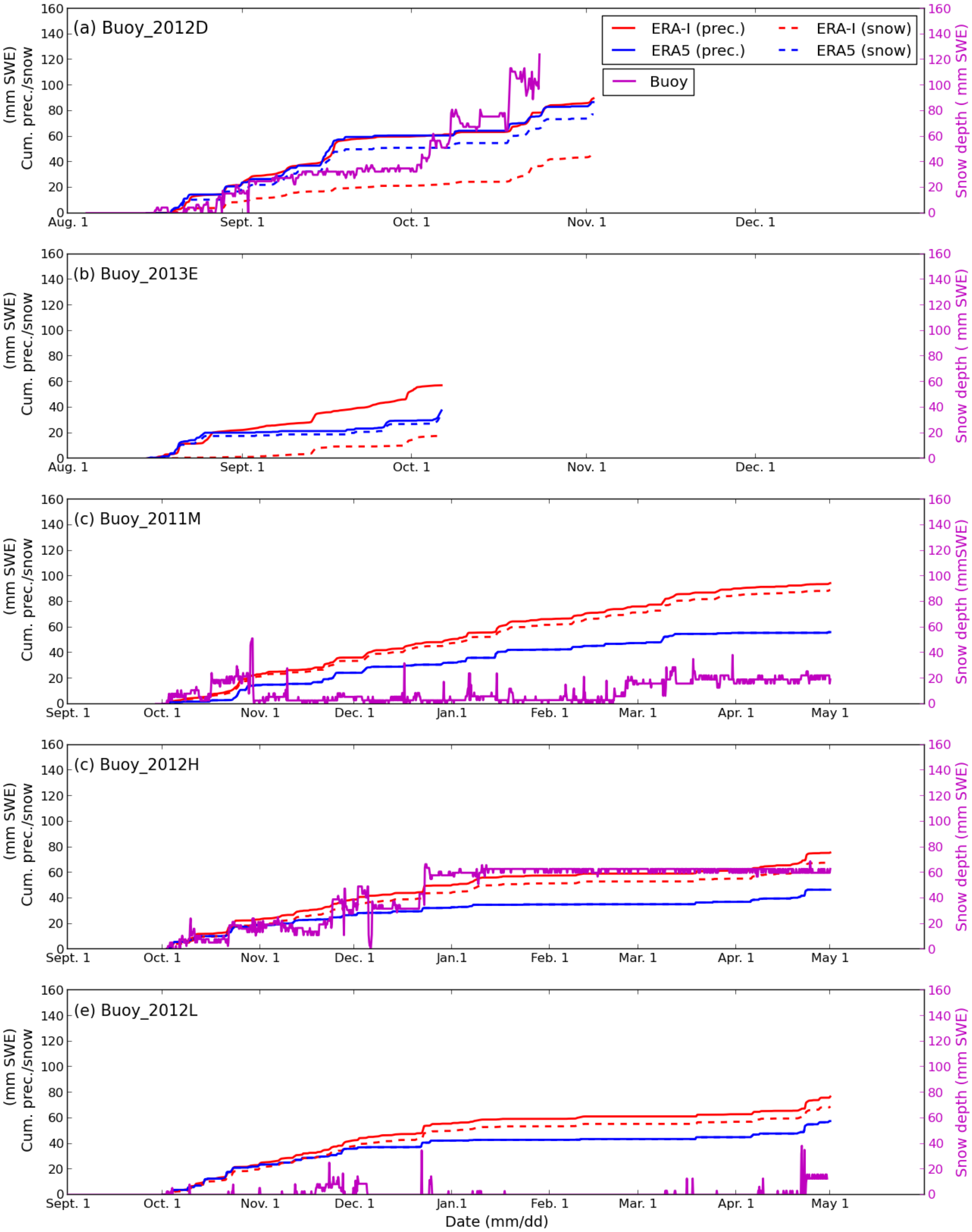

Figure 7. Cumulative total precipitation (prec.) and snowfall (snow) for ERA5 and ERA-I and snow depth for buoys (a) 2012D, (b) 2013E, (c) 2011M, (d) 2012H, and (e) 2012L. Accumulation starts from 15 August for panels (a) and (b) and from 1 October for panels (c)-(e). Note there was no snow depth data for buoy 2013E during the accumulation period.

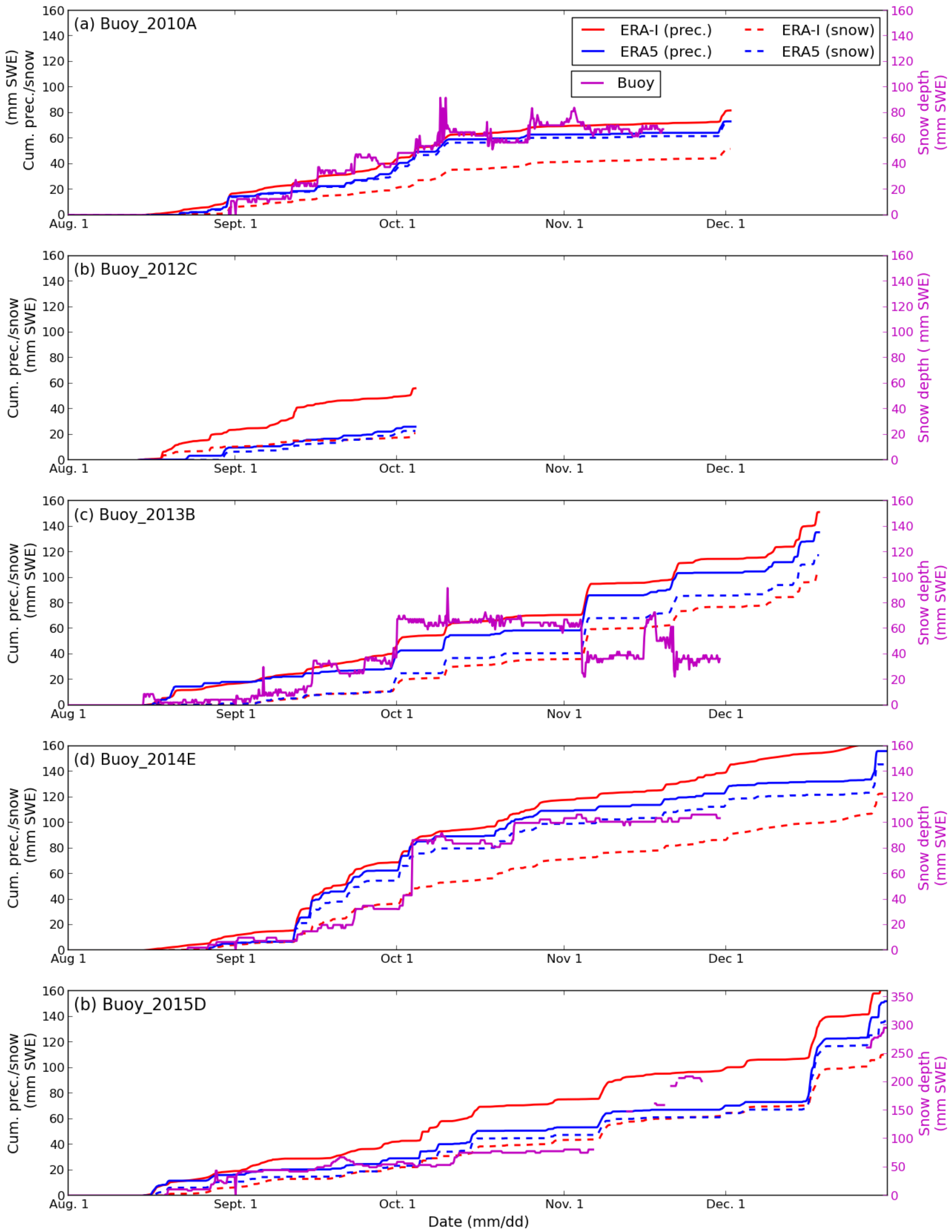

Figure S4. Cumulative total precipitation (prec.) and snowfall (snow) for ERA5 and ERA-I and snow depth from for buoys (a) 2010A, (b) 2012C, (c) 2013B, (d) 2014E, and (e) 2015D. Accumulation starts from 15 August. Note that Buoy_2012C does not have snow depth.

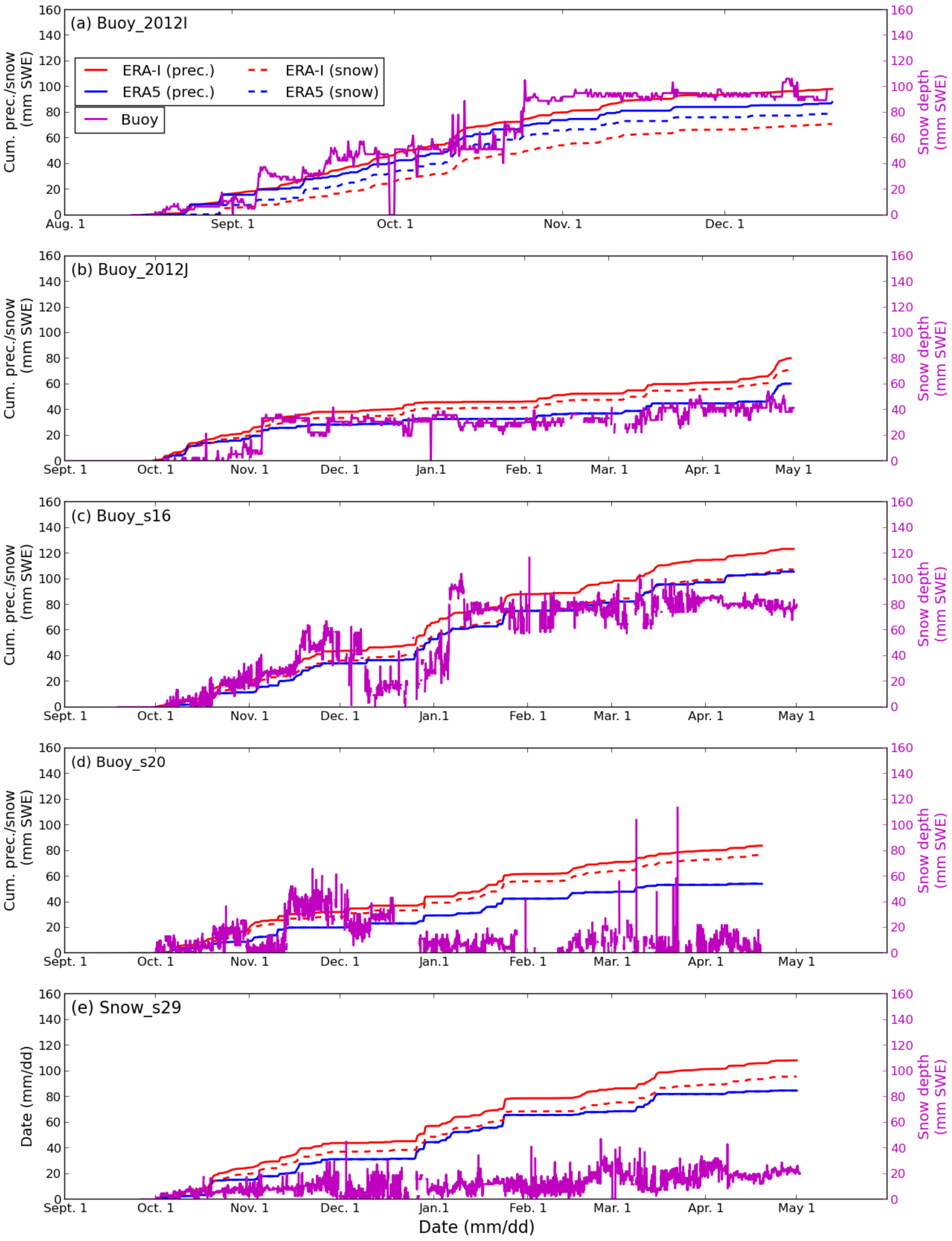

Figure S5. Same as Figure S4, but for buoys (a) 2012I, (b) 2012J, (c) s16, (d) s20, and (e) s29, and accumulation starts on 1 October.

Line 18 page 6 should be ERA5

It was corrected to ERA5.

Comparison of ERA5 and ERA-Interim near surface air temperature and precipitation over Arctic sea ice: Effects on sea ice thermodynamics and evolution

Caixin Wang[1, 2], Robert M. Graham[2], Keguang Wang[1], Sebastian Gerland[2], Mats A. Granskog[2]

[1]Norwegian Meteorological Institute, ~~Tromsø,~~ 9293~~,~~ Tromsø, Norway

[2]Norwegian Polar Institute, Fram Centre, ~~Tromsø, 9296,~~ P.O.Box 6606 Langnes, 9296 Tromsø, Norway

Correspondence to: Caixin Wang (caixin.wang@npolar.no)

Abstract. Rapid changes are occurring in the Arctic, including a reduction in sea ice thickness and coverage and a shift towards younger and thinner sea ice. Snow and sea ice models are often used to study these ongoing changes in the Arctic, and are typically forced by atmospheric reanalyses in absence of observations. ERA5 is a new global reanalysis that will replace the widely used ERA-Interim (ERA-I). In this study, we compare the 2 m air temperature (T2M) and precipitation ~~between~~ from ERA-I and ERA5, and evaluate these products using buoy observations from Arctic sea ice for years 2010 to 2016. We further assess how biases in reanalyses can influence the snow and sea ice evolution in the Arctic, when used to force a thermodynamic sea ice model. We find that ERA5 is generally warmer than ERA-I in winter and spring, but colder than ERA-I in summer and autumn over the pan-Arctic sea ice. ~~both~~ Both reanalyses have a warm bias over Arctic sea ice in relation to the buoy observations. The warm bias is smaller in the warm season, and larger in the cold season, especially when the T2M is ~~lower than~~below -25°C in the Atlantic and Pacific sectors. Interestingly, the warm bias in the new ERA5 is on average 2.1 °C (daily mean) larger than ERA-I during the cold season. While ERA-I is drier than ~~most~~ some modern reanalyses in the Arctic, the total precipitation along the buoy trajectories and over the pan-Arctic sea ice is often lower in ERA5 than in ERA-I. Nonetheless, the snowfall products are broadly similar for both ERA-I and ERA5. ERA-I ~~had~~ has substantial anomalous Arctic rainfall, which is greatly reduced in ERA5. Simulations with ~~a freezing degree days (FDD) model and~~ a 1D thermodynamic sea ice model demonstrate that the warm bias in ERA5 acts to reduce thermodynamic ice growth. However, the lower precipitation in ERA5 results in a thinner snow pack that allows more heat loss to the atmosphere. Thus, the larger warm bias and lower precipitation in ERA5, compared with ERA-I, compensate in terms of the effect on winter ice growth. Ultimately, we find slightly thicker ice at the end of growth season when using ERA5 forcing, compared with ERA-I. Thus differences in ~~the~~ precipitation ~~fields~~ of the two reanalyses have a larger influence on the sea ice evolution than ~~the~~ T2M.

1 Introduction

The Arctic has been undergoing substantial changes in the recent decades. The decline of Arctic sea ice is seen as one of the most prominent indicators of Arctic climate change (Stroeve et al., 2012). The extent and area of the Arctic sea ice has decreased (Comiso et al., 2008), the length of the sea ice melt season is increasing (Markus et al., 2009; Mortin et al., 2014; Stroeve et al., 2014; Mortin et al., 2016; Stroeve and Notz, 2018), and large areas of thick multi-year ice (MYI) have been replaced by thinner and more dynamic first-year ice (FYI) (Maslanik et al., 2011; Lindsay and Schweiger, 2015; King et al., 2017). ~~The decline of Arctic sea ice has been attributed to various interrelated causes, including a general overall warming trend (Steel et al., 2008; Polyakov et al., 2010).~~ The Arctic is warming more than twice as fast as the global average temperature over the past 50 years (Bekryaev et al., 2010; AMAP, 2017). The fastest warming in the Arctic occurs during the fall and winter season (Graversen et al., 2008; Boisvert and Stroeve, 2015), and is driven in part by an increased number of storms that bring warm winds from the south (Woods and Caballero, 2016; Dahlke and Maturilli, 2017; Graham et al., 2017a, 2017b; Rinke et al., 2017). The additional heat and moisture carried by these storms could contribute to a reduction in the winter ice growth (Woods and Caballero, 2016; Alexeev et al., 2017; Stroeve et al., 2018).

Despite the rapid ongoing changes in the Arctic, there are relatively few ~~in-situ atmospheric~~direct observations of the atmosphere, sea ice and ocean conditions, especially during winter. Due to the lack of in-situ observations, most studies documenting changes in the Arctic rely heavily on atmospheric reanalyses (Screen and Simmonds, 2010; Kapsch et al., 2014; Woods and Caballero, 2016; Sato and Inoue, 2017). In addition, ~~Atmospheric~~ reanalyses are also ~~often~~frequently used to force snow and sea ice models (Schweiger et al., 2011; Merkouriadi et al., 2017; Stroeve et al., 2018). However, there are inherent biases and uncertainties within these reanalyses, and large differences can exist among the different products (Tjernstöm and Graversen, 2009; Decker, et al., 2012; Jakobson et al., 2012; Lindsay et al., 2014; Wesslén et al., 2014; Graham et al., 2017b). ~~Atmospheric reanalyses are often used to force snow and sea ice models (Schweiger et al., 2011; Merkouriadi et al., 2017; Stroeve et al., 2018).~~ Thus the choice of reanalysis, and inherent biases within that product, will ultimately influence the simulation of Arctic sea ice mass balance (Cheng et al., 2008; Wang et al., 2015).

The European Centre for Medium-range Weather Forecasts (ECMWF) reanalysis product, ERA-Interim (ERA-I, Dee et al., 2011), has been widely used for studying changes in the Arctic and forcing ocean and sea ice models (e.g., Cheng et al., 2008; Maksimovich and Vihma, 2012; Kapsch et al., 2014; Woods and Caballero, 2016; Graham et al., 2017b). In 2017, the ECMWF released a new reanalysis ~~data~~ ERA5 (Hersbach and Dee, 2016). There are several major improvements in ERA5 compared with ERA-I~~. For example, ERA5 covers a longer period from 1950 (ERA-I from 1979) to present~~, including ~~has~~ much higher spatial and temporal resolutions, ~~includes more information on variation in quality over space and time, an improved representation of troposphere, better global balance of precipitation and evaporation,~~ and more consistent sea surface temperature and sea ice ~~coverage~~ concentration (Hersbach and Dee, 2016). Evaluations of the performance of ERA5 have been conducted over the land and revealed a higher performance of ERA5 than ERA-I (Albergel et al., 2018; Urraca et al., 2018), and other commonly used reanalysis, such as, MERRA-2 (the second version of the Modern-Era Retrospective Analysis for

Research and Applications) (Olausen, 2018; Urraca et al., 2018). However, the performance of ERA5 over Arctic sea ice is yet to be fully investigated.

In this study, we compare and evaluate the performance of ~~2 m air temperature (T2M) and precipitation in~~ ERA-I and ERA5 over Arctic sea ice. ~~These are both critical parameters for sea ice simulation (Cheng et al., 2008; Wang et al. 2015). To evaluate the two reanalysis products~~For this, we use data from Ice Mass Balance buoys (IMB) (Perovich et al., 2018) and Snow Buoys (Grosfeld et al., 2016; Nicolaus et al., 2017) deployed in 2010 to 2015. The~~se~~ buoys ~~typically~~ record position, the 2 m air temperature (T2M), mean sea level pressure (MSLP), and snow depth at regular intervals ~~(from hourly to every four hours)~~. Hence, these observations can be used to evaluate the variables of T2M, precipitation and MSLP in the reanalyses. The~~se~~ former two variables are ~~both~~ critical parameters for sea ice simulation (Cheng et al., 2008; Wang et al. 2015), and form the focus of our study.~~.~~ We use the T2M and snow depth observations from these buoys to assess the performance of ERA5 and ERA-I over Arctic sea ice. We further ~~apply a freezing degree day (FDD) model to both reanalyses, and~~ use the reanalyses to force a 1-D thermodynamic sea ice model. The simulations are compared with snow and ice thickness observations from the buoys to evaluate how differences in the T2M and precipitation influence the evolution of sea ice in the model.

2 Materials and Methods

2.1 Buoy data

IMBs autonomously measure thermodynamic changes in sea ice mass balance (Richter-Menge et al., 2006; Polashenski et al., 2011). They are part of a network of drifting buoys over the Arctic Ocean that provide meteorological and oceanographic data for real-time operational requirements and research purposes (Rigor et al., 2000). These instruments typically record GPS position, T2M and mean sea level pressure (MSLP) at hourly intervals, ~~and~~ as well as temperature profiles through the air, snow, ice, and upper-ocean, and distances to snow/ice surface and ice bottom at ~~every~~ four hour intervals. Snow depth and ice thickness can be estimated from the distances measured by acoustic sounders, if ~~knowing~~ the initial thickness of snow and ice are known when the IMB is deployed (Wang et al., 2013). If the acoustic sounders fail but the temperature string works, the positions of the ice surface and bottom can be determined from the temperature readings. Similar to IMBs, Snow Buoys also record GPS position, T2M, MSLP, and snow depth at hourly intervals (Grosfeld et al., 2016; Nicolaus et al., 2017). However, Snow Buoys do not measure temperature profiles, and provide no information on ice thickness.

Since 2000, a large number of IMBs have been deployed across the Arctic, in regions such as the Central Arctic, the Beaufort Sea, the Chukchi Sea, the Laptev Sea, the North Pole, Canadian Islands and Svalbard (Perovich et al., 2018) (http://imb-crrel-dartmouth.org/archived-data/). In this study, we use data from 13 IMBs deployed in these different regions between 2010-2015 (Fig. 1, Table 1). The IMBs were typically deployed in the Central Arctic during April/May, while deployments in the Beaufort, the Laptev, and Chukchi Seas generally took place in August/September (Fig. 1, Table 1). For ~~more~~ additional coverage, we also use observations from 3 snow buoys deployed in 2015, two of which in the Laptev Sea and one in the Central

Arctic (Table 1; Fig. 1) (http://www.meereisportal.de/en). For simplicity, hereafter we refer to IMBs and Snow Buoys as buoys.

2.2 ERA5 and ERA-I reanalysis data

ERA5 is the ECMWF's latest reanalysis product, and will replace the widely used ERA-I. The first batch of ERA5, covering the period 2010-2016, was released in July 2017. The entire ERA5 dataset, ~~including~~ extending back to~~the period from~~ 1950 ~~to present, is expected to be~~will be available for use ~~by early~~in late 2019. ERA5 and ERA-I both have global coverage, with a horizontal spatial resolution of 80 km for ERA-I, and 31 km for ERA5. In the vertical, ERA5 resolves the atmosphere using 137 levels from the surface up to a height equalling 0.01 hPa, and ERA-I uses 60 levels from the surface up to an equivalent height of 0.1 hPa. ERA5 provides hourly analysis and forecast fields, while ERA-I provides 6-hourly analysis and 3-hourly forecast fields. For the data assimilation, both apply 4-dimensional variational analysis (4D-var). ERA-I uses the Integrated Forecast System (IFS) "Cy31r2" 4D-Var, and ERA5 applies the newer IFS "Cy41r2" 4D-Var". ERA5 includes various newly reprocessed datasets and recent instruments that could not be ingested in ERA-I. Many new parameters, such as 100 m wind vector, are available as part of the ERA5 output. For comparison and evaluation against buoy observations, ERA5 is bilinearly interpolated to the buoy positions, and ERA-I is first linearly interpolated to hourly data, and then bilinearly interpolated to the buoy positions. For comparison between ERA-I and ERA5 over the Arctic sea ice, the ERA-I data are first bilinearly interpolated to the grid of ERA5, and then T2M is averaged in the season, and total precipitation and snowfall is integrated over the season.~~, the ERA-I data here are bilinearly interpolated to the grid of the ERA5, and the ERA-I and ERA5 reanalysis are bilinearly interpolated to the buoy positions.~~

3 Comparison of reanalysis and buoys' near surface air temperature and precipitation ~~against buoy observations~~over the Arctic sea ice

3.1 Spatial distribution of seasonal difference of reanalysis near surface temperature and precipitation

Figure 2 shows the seasonal mean differences of T2M, total precipitation and snowfall between ERA5 and ERA-I over Arctic sea ice during 2010-2015. We classify spring as March, April and May, summer as June, July and August, autumn as September, October and November, and winter as December, January and February. The seasonal mean ice extent is obtained from the monthly sea ice concentration from NOAA/NSIDC during 2010-2015 (Meier et al., 2017).

The difference in T2M between ERA5 and ERA-I clearly varies with season (Fig. 2a-d). ERA5 is generally warner than ERA-I in spring and winter, and colder than ERA-I during summer and autumn over most regions of Arctic sea ice. These temperature differences are small during summer, but large during the other seasons. Near the North Pole, ERA5 is warmer than ERA-I in summer, but colder than ERA-I in winter. Whether warmer or colder, the differences between ERA5 and ERA-I are small (<±0.4 °C) in this region.

ERA-I is known to be a relatively “dry” global reanalysis product in the Arctic compared with most other modern reanalyses (e.g. MERRA-2, CFSR, and JRA-55) (Lindsay et al., 2014; Merkouriadi et al., 2017; Boisvert et al., 2018). However, the total precipitation in ERA5 is lower than in EAR-I over Arctic sea ice in all seasons (Fig. 2e-h). The lower precipitation in ERA5 is most pronounced in summer, and in the eastern Arctic. Differences in the snowfall between ERA5 and ERA-I are smaller than for total precipitation (Fig. 2 i-j vs. Fig. 2e-h). The snowfall in ERA5 is lower than in ERA-I in spring, autumn and winter, but larger than ERA-I in summer.

3.1 Comparison of reanalysis near surface temperature against buoy observations

Both ERA-I and ERA5 accurately capture the observed evolution of MSLP measured by each of the buoys (not shown). The hourly difference between the reanalysis MSLP and observations is no more than a few hPa. Excellent agreements between observed MSLP in the Arctic and earlier reanalyses have been shown in previous studies (e.g, Makshtas et al., 2007), demonstrating that MSLP is well simulated in reanalyses. In the following, we will focus on near surface temperature and precipitation.

3.2.1 Evaluation of near surface temperature in ERA5 and ERA-I using buoy observations

~~**3.1 Evaluation of near surface temperature in ERA5 and ERA-I using buoy observations**~~

Figure 3~~2~~ and Figures S1-2~~3~~ show time series of T2M from different buoys, and the corresponding T2M difference between~~from~~ ERA5 and ERA-I at the buoys’ positions. The observed T2M reveals the pronounced seasonal cycle in the Arctic. Low temperatures persist through winter ~~(January - March)~~ and spring ~~(April - June)~~, before approaching near 0ºC around the end of May or early June. Temperatures near 0ºC, or occasionally over 0ºC, continue during summer ~~(July - September)~~, before lower temperatures return in late August or early September and decrease further in autumn ~~(October - December) (Fig. 2 & 3)~~.

The T2M in ERA5 and ERA-I generally agree well, both with each other and the observations (Figs. 3~~2~~ & S1-2~~3~~). The reanalyses perform best for ~~the~~ buoys ~~of~~ 2013E (Fig. ~~2d~~3b), and 2012J (Fig. ~~3d~~S2b), which were both deployed in the central Arctic, the former near the North Pole and the later closer to the Laptev Sea (Fig. 1). ~~However, o~~On occasions, hourly differences of T2M between ERA5 and ERA-I can ~~be up to 8~~exceed 4 ºC (e.g., ~~Fig. 2g and~~ Fig. 3~~a-~~c-e). The largest hourly T2M differences between the two reanalyses (Fig. 3 & Figs. S1-S2), and between the reanalyses and observations (Fig. 4 & S3), are found during the coldest months (November–May). Specifically, both reanalyses have a warm bias during these months. Previous studies have shown that warm biases in the Arctic are prevalent among most reanalysis products, particularly during the winter season (Beesley et al., 2000; Tjernstöm and Graversen, 2009; Lüpkes et al., 2010; Jacobson et al., 2012; Lindsay et al., 2014; Wesslén et al., 2014; Graham et al., 2017b). This is because weather forecast models and climate models struggle to accurately simulate strong stable boundary layers (Beesley et al., 2000; Tjernstöm and Graversen, 2009;

Sotiropoulou et al., 2015; Graham et al., 2017b; Kayser et al., 2017; Biosvert et al., 2018). Interestingly, we find a larger warm bias in the new ERA5 compared with ERA-I (Fig. ~~2~~4 & S3, Table 2), despite the higher vertical resolution in ERA5.

We note that the near surface air temperature in both reanalyses corresponds to a height of 2 m, while it is typically measured by buoys at a height of about 1.0-1.5 m above the surface, when the buoys ~~are~~ were installed. The initial~~1.0 m~~ observation height might decrease further as snow accumulates during the cold season. During winter, the lowest temperatures in the Arctic occur under stable conditions with a strong surface-based inversion, meaning that the temperature increases with height from the surface. Hence, the near surface warm bias in reanalyses may partly be attributed to the difference in height with the observations (Vihma et al., 2014).

A scatterplot of ~~the~~ ERA5/ERA-I vs. buoy~~'s~~ T2M clearly reveals the temperature dependence of the warm bias in both reanalyses (Fig. 5~~4~~a). The data crowd together near the 1:1 line when the air temperature is near 0°C, but spread further above the 1:1 line when the air temperature is low, especially at air temperatures below -25°C. The temperature dependence of the warm bias is also demonstrated in Fig. 5~~4~~b, which shows the relationship between the daily mean T2M differences with the temperature bins of 5 °C from -45 – +5 °C. When the T2M is below -25 °C, the daily mean difference between reanalysis and observation is more than 2 °C, with ERA5 3.1 – 8.0 °C warmer than in buoys, and ERA-I 2.4 – 4.4 °C warmer than in buoys (Fig. ~~4~~5b). For air temperatures above -25 °C, the bias between reanalysis and buoys is smaller, with ERA5 and ERA-I both 0.75 °C warmer than the observations on average.

Figure 5~~4~~c shows the bias and standard deviation (std) for the reanalyses for each month, based on the buoy observations, and the temperature difference between the reanalyses. The smallest biases, and the smallest T2M differences between ERA5 and ERA-I are found in the months between July and October (also refer to Fig. 3-4~~2~~ & S1-S3). ERA5 is typically warmer than ERA-I (and has a larger warm bias) throughout the winter and spring, including June. However, ERA5 ~~was~~ is colder than ERA-I (0.01-0.6 °C), and has smaller biases from July - October (Fig. 5~~4~~c). Hence, the warm bias in ERA5 is smaller than ERA-I in the warm season (July-October). ERA-I has a warm bias in the warm season, but the ~~bias~~ magnitude is smaller (< 0.8 °C) ~~compared with~~ than~~t~~ the warm bias in the cold season (Fig. ~~4~~5c). Similarly, ERA5 has a small warm bias during July and August (<1 °C), and a likely insignificant cold bias (< 0.2 °C) in September and October (Fig. ~~4~~5c).

The performance of reanalysis near surface temperature varies with region over Arctic sea ice (Fig. 6, also refer to Fig. 2). According to the buoys' positions (Fig. 1), we define four regions in the Arctic: the Central Arctic (north of 86° N), and the Pacific sector (90° W – 150° E), the Atlantic sector (30° W – 60° E), and the Laptev Sea (60° E – 150° E). The later three sectors are south of 86° N. The ERA5/ERA-I near surface temperature performs best in the Central Arctic (Fig. 6a), and well in the Pacific sector (Fig. 6c). It performs well in the Atlantic sector when the T2M is above -25 °C, but poorly when the T2M is below -25 °C (Fig. 6b). The performance of reanalysis near surface temperature in the Laptev Sea needs to be further investigated due to small number of observations in this region (Fig. 6d & 6h). However, there is also some seasonal bias in the availability of data from buoys in the different regions, largely due to when buoys are deployed in different regions of the Arctic and ice drift patterns.

3.2.2 Comparison of precipitation and snowfall from ERA5 and ERA-I along buoy drift trajectories

~~3.2 Comparison of precipitation and snowfall from ERA5 and ERA-I along buoy drift trajectories~~

We next compare the cumulative total precipitation and snowfall in ERA5 and ERA-I in autumn and winter, along the drift trajectories of the buoys. We begin accumulating the precipitation from 15 August onwards if the buoy was deployed before this date~~ (Fig. 5)~~, or from 1 October if the buoy was installed after 15 August~~ (Fig. 6)~~. We accumulate the precipitation until 30 April, or the end of operation if the buoy stopped working before 30 April in the respective years (see Table 1).

The accumulated total precipitation in ERA5 is lower than ERA-I for each of the analysed buoys (Figs. ~~5 & 6~~7 & S4-5, and Table 1), which is consistent with the seasonal difference in total precipitation documented in section 3.1 (Fig. 2e-h). On average, the accumulated total precipitation in ERA-I is 19.5 mm water equivalent larger than in ERA5, with differences for the individual buoys ranging from 2.0 (buoy 2012D; Fig. ~~5c~~7a) to 38.4 mm water equivalent (buoy 2011M; Fig. ~~6a~~7c). This is ~~interesting~~indicates that ERA5 is drier than ERA-I, which is ~~because ERA-I is~~ known to be a relatively "dry" global reanalysis product in the Arctic compared with most other modern reanalyses (e.g. MERRA-2, CFSR, and JRA-55) (Lindsay et al., 2014; Merkouriadi et al., 2017; Boisvert et al., 2018).

Unlike the accumulated total precipitation, the accumulated snowfall (~~Sf~~SF) in ERA5 is sometimes ~~can be~~ larger than that in ERA-I (Figs. ~~5~~ 7 & ~~6~~S4-5; Table 1). Specifically, ~~F~~for buoys deployed near the North Pole~~, which~~ that started operating on 15 August, the accumulated ~~Sf~~ SF in ERA5 is typically larger than ERA-I~~.~~ (Fig. ~~5~~7a-b & S4, S5a). In contrast, for buoys deployed in other regions, which started operating on 1 October, the accumulated snowfall in ERA5 is typically lower than ERA-I (Fig. 7c-e & Figs. S5b-e~~6~~).

The ratio of snowfall to precipitation in ERA5 is relatively high, meaning that most of the total precipitation falls as snow in ERA5. In contrast, ERA-I has a relatively low snowfall to precipitation ratio, especially during August-September. ~~Hence,~~This means that substantial precipitation falls as rain in ERA-I during August-September, ~~while~~ but the same precipitation events in ERA5 are classified as snowfall. This difference in snowfall to precipitation ratio can help to explain~~s~~ why the accumulated snowfall in ERA5 is greater than ERA-I for buoys deployed in August, but ~~less~~ lower than ERA-I for buoys starting in October. The low snowfall to precipitation ratio and thus larger fraction of rainfall in ERA-I is known to be anomalous, and is likely due to the cloud physics scheme used (e.g., Dutra et al., 2011; Leeuw et al., 2015). In ERA-I, the split between liquid and ice in clouds is determined diagnostically as a function of temperature from -23 to 0 °C, with ice-only only below -23 °C and liquid-only above 0 °C. In contract, the IFS Cy41r2 used in ERA5 includes a prognostic microphysics scheme, with separate cloud liquid, cloud ice, rain and snow prognostic variables (Sotiropoulou et al., 2015; see also ECMWF IFS documentation – Cy41r2; https://www.ecmwf.int/sites/default/files/elibrary/2016/16648-part-iv-physical-processes.pdf). Our findings indicate that ERA5 has significantly less ~~anomalous~~ Arctic rainfall than ERA-I, particularly in August-September (Fig. 7, Figs. S4-5).

Evaluating the performance of precipitation products over the Arctic Ocean is a major challenge due to the lack of observations, and difficulty accurately measuring snowfall (e.g. Lindsay et al., 2014; Rasmussen et al., 2012; Sato et al., 2017;

Blanchard-Wrigglesworth et al., 2018; Boisvert et al., 2018; Webster et al., 2018). Here we compare the precipitation from ERA-I and ERA5 with snow depth measurements from the buoys (Table 1). For this comparison, snow depth from the buoys is converted to snow water equivalent (SWE) using a climatological monthly ~~assuming a~~ mean snow densities~~y~~ of 220-~~350~~ 380 kg m^{-3} (Warren et al., 1999). The accumulated total precipitation from ERA5 and ERA-I in Fig. ~~5~~7 and Figs. S4-5~~6~~ is converted to SWE assuming that precipitation falls as snow/solid precipitation when the air temperature is below zero (we call this the accumulated ~~Sp~~TP). Caution must be taken here, as the buoys reflect point observations, while the reanalyses provide a grid cell average. Snow depth is known to have large variability even over relatively small spatial scales (Warren et al., 1999; Sturm et al., 2002; Liston et al., 2018). An unknown fraction of the true snow fall will also be lost through blowing snow into leads, which is not accounted for in our calculation~~ below~~.

The accumulated ~~Sp~~ TP and SF from ERA-I and ERA5 ~~is~~are ~~typically~~ generally comparable with the observed SWE from buoys in most cases during the accumulation period, such as buoy 2012H deployed in the Beaufort Sea (refer to Fig. 7 & Figs. 4-5). However, in several cases the accumulated TP and SF from ERA-I and ERA5 considerably lower than the observed SWE from buoys, such as buoy 2012D from mid-October. This may be caused by snow drifting up against the buoy structure, or reflect anomalously low precipitation in the reanalyses. In other cases, the accumulated TP and SF from reanalysis is higher ~~larger on average 38.9 mm SWE for ERA-I and 26.9 mm SWE for EA5 than~~ the observed SWE from buoys during some periods (buoys 2013B and s20) or for the whole accumulation period (buoys 2011M, 2012L and S20)~~, (see Table 1)~~. ~~However, there are cases where the accumulated Sp from both ERA-I and ERA5 was lower (mean: 93.8 mm SWE for ERA-I; 91.6 mm SWE for ERA5) than that from the buoys, which are buoys 2010A, 2012D, 2012I and 2015D deployed in the Central Arctic in April except buoy 2012I. For example, along the buoy 2015D, the accumulated Sp from ERA-I (144.4 mm SWE) and ERA5 (140.2 mm SWE) is much lower than that from the buoy (392.0 mm SWE). This may be due to snow drifting up against the buoy structure, or reflect anomalously low precipitation in the reanalyses. In contrast, along the buoy drift trajectory of 2012L which was deployed in Beaufort Sea in late August, the accumulated Sp from ERA-I (76.9 mm SWE) and ERA5 (57.8 mm SWE) is substantially larger than that from the buoy (14.0 mm SWE).~~ This ~~might~~ could be caused by~~reflect~~ snow erosion/~~ or~~ sublimation a~~t the IMB_2012L site~~round the buoy, or reflect anomalously high precipitation in the reanalyses. By the end of the accumulation period, the accumulated TP/SF is larger on average 55.4/41.9 mm SWE for ERA-I and 38.9/43.7 mm SWE for ERA5 than the observed SWE of the snow pack along the buoy trajectories (see Table 1).

4 Influence of air temperature and precipitation on sea ice evolution during the freezing season

In this section, we evaluate the impact of different forcing products (ERA-I, ERA5, and the buoys) on sea ice evolution. We focus on the freezing/growth season, from 1 October to 30 April, when sea ice generally starts to grow after summer. This period corresponds to the time when the largest differences of T2M between ERA5 and ERA-I were found (Figs. 2-4). For this exercise, we focus on~~ the~~ buoys~~ of~~ 2011M, 2012H, 2012L, and 2012J that were deployed in late August/early September and operated for more than one year, covering a complete freezing season (Table 1). These buoys were installed ~~either~~ on MYI or FYI in the central Arctic (buoy 2011M), the Beaufort Sea (buoy ~~2011M~~2012H, buoy 2012L), or the Laptev Sea (buoy 2012J). When these buoys were installed, sea ice thickness was~~ usually~~ between 1-2 m for buoys 2011M, 2012H, and 2012J, ~~except~~ while buoy 2012L ~~(~~had an ice thickness of 3.35 m (Table 1). Snow depth was typically ~~with~~ a few centimetres of snow at deployment~~(Table 1)~~. We use these buoys to assess the impact of different forcing data on sea ice evolution. For our simple approach we apply ~~an accumulated~~the empirical cumulative freezing degree day (FDD) model, which accounts for differences in T2M, and a 1D sea ice model that also account for effects of precipitation.

4.1 Assessing the sea ice evolution with freezing degree days (FDD): impact of temperature bias

~~Ice growth can be estimated with a~~The cumulative freezing degree days (FDD) model only needs air temperature as input and is often used to estimate sea ice growth (Δh) from zero (e.g., Huntemann et al., 2014; Lei et al., 2017). ~~The FDD is defined as the time-integrated air temperature below the seawater freezing point (-1.8 °C) during the freezing season. It is essentially a measure of how cold it has been for how long, reflecting the atmospheric forcing on sea ice mass balance.~~ The ~~thermodynamic~~ sea ice growth ~~(h), from an initial thickness of 0 m, can be~~is estimated ~~using a simple ice-growth parameterization by~~based on Lebedev (Maykut, 1986), ~~:~~

$$\Delta h = 1.33\sum(FDD)^{0.58}$$ ~~(1)~~

~~While~~ where $\sum FDD$~~snow depth~~ is daily average temperature below the freezing point of sea water (-1.8 °C), integrated over the time period from 1 October to 30 April. ~~not explicitly expressed in Eq. (1), the relation between h and FDD describes ice growth under an average rate of snow accumulation over the Russian sector of the Arctic Ocean (Maykut, 1986).~~

The positive near surface air temperature bias in ERA5 and ERA-I results in a negative ice thickness bias at the end of the growth season. ~~When we compare the integrated FDD for the buoys and reanalyses, we find that t~~The cumulative FDD is ~~largest for buoys, and~~ smallest for ERA5 (Fig. S~~7~~6, Table 2), corresponding to~~. This reflects the warm T2M bias in ERA-I and ERA5, in relation to the buoys, with~~ the largest warm bias in ERA5 during the freezing season. The differences in FDD between ERA5, ERA-I and buoys are large for buoys~~ of~~ 2011M, 2012H and 2012L~~ (Fig. 7a-c)~~, but negligible for buoy 2012J. ~~(Fig. 7d). Hence the differences in sea ice growth over the freezing season, estimated using FDD from ERA5, ERA-I and buoys, are large for the former but negligible in case of buoy 2012J (Fig. 7). The negative thickness bias in ERA-I with respect to the FDD calculated using the T2M from the buoys ranges from~~ The ice growth is 0.08-0.12 m less, with a mean of -0.09 m for ERA-I T2M, and ~~. ERA5 has larger ice thickness biases, ranging from~~ 0.13-0.20 m less, with a mean of -0.16 m for ERA5 T2M compared to when using buoy temperatures (Table 2). ~~Hence, the positive near surface air temperature bias in ERA5 and ERA-I results in a negative ice thickness bias at the end of the growth season, when applying this simple FDD model.~~

4.2 Assessing sea ice evolution with a 1D sea ice model HIGHTSI: impact of T2M and precipitation

HIGHTSI is a 1D high-resolution thermodynamic snow and ice model designed for process studies to ~~accurately~~ resolve the evolution of snow/ice thickness and temperature profile. The snow and ice temperature regimes are solved by the partial differential heat conduction equations applied for snow and ice layers, respectively. The turbulent surface fluxes are parameterized taking the thermal stratification of the atmosphere surface layer into account. Downward short- and longwave radiative fluxes are parameterized based on the total cloud cover. The model~~It~~ has been extensively used in Arctic studies (e.g., Cheng et al., 2008; Cheng et al., 2013; Wang et al., 2015; Merkouriadi et al., 2017).

In this section we perform six sensitivity simulations on each of the four buoys to explore the impact of temperature and precipitation on snow and sea ice evolution (Table 3). In the first two simulations, S~~f-ERA~~FI_T2MI and S~~f-ERA~~F5_T2M5, we force HIGHTSI with the T2M, 10 m wind speed (~~U10~~V), relative humidity (Rh), total cloud cover (~~Tcc~~CN) and snowfall, from ERA-I and ERA5 (Fig. S7), respectively. In the next two simulations, ~~Sp-ERA~~TPI_T2MI and ~~Sp-ERA~~TP5_T2M5, we force the model with the total precipitation from the reanalyses, rather than the snowfall, and treat all precipitation as snow when T2M is below 0 °C. This is the same method we used for the accumulated ~~Sp~~ TP in section 3.2. In the final two simulations, we evaluate the influences of T2M and precipitation on the sea ice evolution individually. Specifically, we replace the T2M from ERA-I in the ~~Sp-ERA~~TPI_T2MI run with the T2M from ERA5, and name this run ~~T2M-ERA5_Sp-ERAI~~TPI_T2M5. Similarly, we replace the ~~Sp~~ TP from ERA-I, in the run of ~~Sp-ERA~~TPI_T2MI, with the TP~~Sp~~ from ERA5 for the ~~T2M-ERAI_Sp-ERA5~~TP5_T2MI run (see Table 3). For all of the simulations we apply ~~the same~~a seasonally variant ocean heat flux according to McPhee et al. (2003), which is large in October (10-20 Wm^{-2}), and decreases to nearly zero from mid-November (see Fig S7 IV). Snow-ice, an ice type formed at ice surface (e.g., Leppäranta, 1983), was recently found to significantly contribute to the Arctic sea ice mass balance in a region with thick snowpack on relatively thin ice pack (Granskog et al., 2017; Merkouriadi et al., 2017). A few (1.5-3) millimetres snow-ice formed only in the ~~Sp-ERA~~TPI_T2MI and ~~T2M-ERA5_Sp-ERAI~~TPI_T2M5 runs for buoy 2012J (with the lowest initial ice thickness of all buoys examined, Table 1). This is negligible for the total ice mass balance. Thus, the effect we examine solely depends on the differences in T2M and precipitation on thermodynamic ice growth.

The pattern of snow accumulation recorded by many buoys is consistent with observations by Warren et al. (1999). Namely, they record snow accumulation in late fall, followed by a relatively constant snow depth from December/January–March, and sometimes a late increase in snow depth in early spring (Fig. 8). For example, the observed snow depth at buoy 2012H increased to about 0.25 m in late December, and changed marginally thereafter (Fig. 8a). Similarly, the observed snow depth at buoy 2012L increased from 0.03 m to 0.13 m from early October to mid-November, and then remained around 0.10 m until the end of April (Fig. 8c). Most buoys recorded an increase in ice thickness from early December to the end of the freezing season. For example, the sea ice growth for buoy 2012H began in early December, at a rate of approximately 0.5 cm/d, until late March, and afterward the growth became sluggish at a rate of 0.16 cm/d until the end of April (Fig. 8a). However, buoy 2012L, which had an initial ice thickness of ~ 3.3 m, showed no significant growth until early February, before undergoing a slight increase from around 3.3 m to 3.5 m by the end of the freezing season (Fig. 8c). Sea ice growth for buoy 2011M (Fig. 8b) and 2012J (Fig. 8d) showed a staircase pattern since the ice thickness was derived from measured temperature profile due to the failure of acoustic sounders as mentioned in section 2.1.

We first compare the simulations ~~Sp-ERA~~TPI_T2MI and ~~Sp-ERA~~TP5_T2M5. Differences in the ice thickness at the end of the growth season for the ~~Sp-ERA~~TPI_T2MI and ~~Sp-ERA~~TP5_T2M5 simulations are relatively small, despite the larger warm bias in ERA5 (Fig. 8). In fact, the sea ice was marginally thicker (0.001-0.03 m) in ~~Sp-ERA~~TP5_T2M5 compared with ~~Sp-ERA~~TPI_T2MI for three buoys, and just 0.004 m thinner for buoy 2012L (Fig. 8c). The major differences we see between these simulations is in the snow depth (Fig~~s~~. 8). ~~Sp-ERA~~TPI_T2MI has a deeper snow pack than ~~Sp-ERA~~TP5_T2M5 for all four buoys, ranging from 0.02-0.09 m. This is due to the higher total precipitation in ERA-I, compared with ERA5 (See section 3.2).

In contrast, when HIGHTSI is forced with the reanalyses snowfall product (S~~f-ERA~~FI_ERAI and S~~f-ERA~~F5_ERA5) the differences in snow depth are relatively small, compared with the simulations forced by the total precipitation (~~Sp-ERA~~TPI_T2MI and ~~Sp-ERA~~TP5_T2M5). The S~~f-ERA~~FI_T2MI runs typically have a deeper snowpack (on average 0.02 m) than S~~f-ERA~~F5_T2M5. However, the snow depth in S~~f-ERA~~FI_T2MI is thinner (by 0.03 m on average) and ice thickness is greater (about 0.01 m) than the ~~Sp-ERA~~TPI_T2MI runs (Fig. 8). This is because there is substantial rain at sub-zero temperatures in the S~~f-ERA~~FI_T2MI runs that is classified as snow in the ~~Sp-ERAI~~TPI_T2MI runs. There are no large differences between the snow depth and sea ice thickness at the end of the growth season for the S~~f-ERA~~F5_T2M5 and ~~Sp-ERA~~TP5_T2M5 runs because, unlike in ERA-I, there is little rain at sub-zero temperatures for S~~f-ERA~~F5_T2M5.

We now look at the effect of T2M differences between ERA5 and ERA-I, and compare the ~~T2M-ERA5_ Sp-ERAI~~TPI_T2M5 runs vs. ~~Sp-ERAI~~TPI_T2MI runs (Fig. 9). When using the T2M from ERA5 and not altering the precipitation forcing, the snowpack remains unchanged from the Sp-ERAI runs. However, we find a slightly thinner ice at the end of freezing season, compared with ~~Sp-ERA~~TPI_T2MI runs (on average 0.01 m thinner), as a result of the larger warm bias in ERA5 which slows down the growth of sea ice. This is consistent with our results from the FDD model in Section 4.1.

Finally, we look at the effect of precipitation by comparing the ~~T2M-ERAI_Sp-ERA5~~TP5_T2MI and ~~Sp-ERAI~~TPI_T2MI runs. The snowpack in ~~T2M-EARI_Sp-ERA~~TP5_T2MI is thinner (on average 0.03 m), while the ice thickness is thicker (on average 0.02 m) than that in the ~~Sp-ERA~~TPI_T2M runs (Fig. 9). The thinner snowpack, is due to the lower precipitation in ERA5 compared with ERA-I. This thinner snowpack allows more heat loss to the atmosphere, which results in greater ice growth.

Referring back to the ~~Sp-ERA~~TPI_ERAI and ~~Sp-ERA~~TP5_T2M5 simulations, we see that lower precipitation and thinner snowpack when using ERA5 as forcing data compensates for the larger T2M warm bias in ERA5, compared with ERA-I. Overall, these compensating biases result in comparable ice thickness at the end of the growth season for both reanalyses.

In general, HIGHTSI reproduces the evolution of snow and sea ice observed by the buoys well during the freezing season (Fig. 8-9) although there are some differences. For the snowpack, there was a 10 cm increase in snow depth for IMB_2012H during late December, which seems not well captured by any of the reanalyses~~ (Fig. 6b)~~ and therefore by any the simulations (Fig. 8a & 9a). The simulations for IMB_2012H show an increase in snow depth at the end of April, indicating a snowfall event in the reanalysis. However, this was not recorded by the buoy. Thus, ~~a good representation of precipitation~~not only the magnitude but also the frequency of the precipitation in the reanalysis data ~~seems~~ is crucial for the snow evolution in the simulation~~, not only the magnitude, but also the frequency of the precipitation~~. The representation of snow in the model may further influence the simulated ice thickness (e.g., Fig. 8a). Evaluating precipitation in the Arctic is however challenging as mentioned previously due to the large local variability and lack of representative in-situ observations (e.g., Liston et al., 2018). Differences in the modelled sea ice thickness from the buoy observations in part arise from not knowing the local ocean heat flux at each individual buoy, however, our approach is here to look at the sensitivity relative to the differences in T2M and precipitation in the reanalyses.

5. Conclusions

Atmospheric ~~R~~reanalysis~~ data~~ are often used to force snow and sea ice models. The accuracy of these forcing products is paramount for the reproduction of the sea ice evolution in the model. ERA5 is a new global reanalysis product from ECMWF and will replace the widely used ERA-I. Here we compare the 2 m air temperature (T2M) and precipitation in ERA5 and ERA-I, and evaluate these products against in-situ observations from drifting buoys (IMBs and Snow Buoys) over Arctic sea ice.

Overall, we find~~There is~~ a warm bias in ~~both~~ ERA-I and ERA5, when compared with the buoys~~,~~. In both reanalysis, these bias are ~~which is smallest~~ smallest in summer months, and large~~st~~r during the autumn, winter and spring. The warm bias in ERA5 is smaller than ERA-I during the summer months. However, we ~~found~~ find a larger warm bias in ERA5 than in ERAI during the cold season, especially when the observed T2M was lower than ~~–~~-25 °C in the Atlantic sector and Pacific Sector. For days when the observed T2M was <-25 °C, the daily mean difference between the reanalyses and buoys was, on average, +5.4 °C for ERA5 and +3.4 °C for ERA-I. The near surface warm bias in ERA5 and ERA-I may partly be attributed to the difference in height with observations. The larger warm bias in ERA5 during cold periods ~~indicates~~ suggests this reanalyses ~~still~~ also struggles to accurately simulate strong stable boundary layers, which frequently appear in winter and early spring, despite the higher vertical resolution compared with ERA-I (e.g., Beesley et al., 2000).~~ Nonetheless, in the summer months, the warm bias in ERA5 (less than 0.2 °C) was smaller than ERA-I.~~

The total precipitation over Arctic sea ice in ERA5 was lower than in ERA-I ~~along the buoy drift trajectories~~in all seasons. This is surprising, as ERA-I is known to be drier in the Arctic compared with some other recent reanalyses (Lindsay et al., 2014; Merkouriadi et al., 2017; Boisvert et al., 2018). However, the snowfall is higher in ERA5 than in ERA-I during the summer months. This indicates that ERA5 has a higher snowfall to precipitation ratio than ERA-I during summer. ERA-I ~~has~~ is known to have an anomalously large fraction of liquid precipitation and low snowfall to precipitation ratio in the Arctic, especially during August-September (Dutra et al., 2011; Leeuw et al., 2015)~~, which is not present in ERA5~~. The total precipitation accumulated along the buoys drift trajectories, during the cold season (from 15 August/1 October until a buoy fails or until 30 April), was lower in ERA5 than in ERA-I for every buoy. Similarly, the accumulated snowfall in ERA5 is lower than in ERA-I for all buoys with an accumulation date starting from 1 October. ~~The snowfall component of precipitation are in better agreement between the two reanalyses than the total precipitation.~~ In contrast, the total accumulated snowfall in

ERA5 is higher than in ERA-I for buoys with an accumulation date starting from 15 August, due to likely anomalous summer/autumn rainfall in ERA-I being classified as snow in ERA5. The accumulated total precipitation and/or snowfall ~~solid precipitation (Sp)~~ in ERA5 ~~is~~ are often closer to the SWE content of buoy measured snow pack, compared with ERA-I. ~~However~~ Nonetheless, the lack of representative in-situ observations and difficulty in measuring snow accumulation on sea ice in the Arctic makes it a challenge to accurately evaluate precipitation products over sea ice (e.g. Rasmussen et al., 2012; Lindsay et al., 2014; Sato et al., 2017; Blanchard-Wrigglesworth et al., 2018; Boisvert et al., 2018). ~~Nonetheless,~~Given snow is such a critical factor in sea ice evolution, ~~and therefore~~ more representative observations are therefore needed (e.g. Merkouriadi et al., 2017; Webster et al., 2018).

The larger warm bias during the ice growth season in ERA5, compared with ERA-I, can result in a lower ice thickness when using this as a forcing product for an ice model or a cumulative FDD model. However, this bias is compensated by the lower precipitation and snowfall in ERA5, from 1 October onwards, which results in a thinner snow pack that allows more heat loss to the atmosphere. Overall, using a 1D thermodynamic sea ice model simulations with ERA5 had a slightly larger ice thickness compared with ERA-I at the end of the growth season, despite the larger warm bias in ERA5. Hence, ~~C~~compared with the T2M differences between these two reanalyses, precipitation differences have~~d~~ a greater influence on the snow and ice evolution. More observations of precipitation ~~/~~and snow ~~data~~ on sea ice are ~~clearly~~ required to ~~properly~~ further evaluate ~~reanalyses~~ reanalysis precipitation in the central Arctic.

Authors contributions

CW, KW and MAG initiated the study. CW and MAG retrieved the buoy data. CW and KW downloaded and analysed the reanalysis data and performed the 1D model simulations. All authors contributed to writing the manuscript.

Acknowledgements

This study was supported by the Research Council of Norway through project SPARSE (project 254765), the Fram Centre “Arctic Ocean” flagship program through the SOLICE project, and by the Centre for Ice, Climate and Ecosystems (ICE) at the Norwegian Polar Institute through the N-ICE project. We wish to acknowledge ECMWF for ERA-Interim and ERA5 data, the International Arctic Buoy Program (IABP) for the IMB data (http://imb-crrel-dartmouth.org/results/), ~~and~~ the Alfred Wegener Institute for Snow Buoy data (http://data.seaiceportal.de/gallery/index_new.php).

References

Albergel, C., Dutra, E., Munier, S., Calvet, J.-C., Munoz-Sabater, J., Rosnay, P., and Balsamo, G.: ERA-5 and ERA-Interim driven ISBA land surface model simulations: which one performs better? Hydol. Earth Syst. Sci, 22, 3515-3532, doi.org/10.5194/hess-22-3515-2018, 2018.

Alexeev, V. A., Walsh, J. E., Ivanov, V. V., Semenov, V. A., and Smirnov, A. V.: Warming in the Nordic Seas, North Atlantic storms and thinning Arctic sea ice, Environmental Res. Lett., 12, 084011, 2017.

AMAP, Snow, Water, Ice and Permafrost in the Arctic (SWIPA) 2017. Arctic Monitoring and Assessment Programme (AMAP), Oslo, Norway, Xiv +269 pp, 2017.

Beesley, J. A., Bretherton, C. S., Jakob C., Anderas, E. L., Intrieri, J. M., and Uttal, T. A.: A comparison of cloud and boundary layer variables in the ECMWF forecast model with observations at Surface Heat Budget of the Arctic Ocean (SHEBA) ice camp, J. Geophys. Res., 105(D10), 12337-12349, doi:10.1029/2000JD900079, 2000.

Bekryaev, R. V., Polyakov, I. V., and Alexeev, V. A.: Role of polar amplification in long-term surface air temperature variations and modern arctic warming, J. Clim., 23(14), 3888–3906, doi:10.1175/2010JCLI3297.1, 2010.

Blanchard-Wrigglesworth, E., Webster, M. A., Farrell, S. L., and Bitz, C. M.: Reconstruction of snow on Arctic sea ice, J. Geophys. Res., Oceans, 123, 3588-3602, https://doi.org/10.1002/2017JC013364, 2018.

Boisvert, L. N., and Stroeve, J. C.: The Arctic is becoming warmer and wetter as revealed by the Atmospheric Infrared Sounder. Geophys. Res. Lett., 42, 4439–4446, doi:10.1002/2015GL063775, 2015.

Boisvert, L. N., Webster, M. A.,Petty, A. A., Markus, T., Bromwich, D. H., and Cullather R. I.: Intercomparison of precipitation estimates over the Arctic Ocean and its peripheral seas from reanalyses, J. Clim., doi:10.1175/JCLI-D-18-0125.1, 2018.

Cheng, B., Zhang, Z., Vihma, T., Johansson, M., Bian, L., Li, Z., and Wu, H.: Model experiments on snow and ice thermodynamics in the Arctic Ocean with CHINARE 2003 data, J. Geophys. Res., 113, C09020, doi: 10.1029/2007JC004654, 2008.

Cheng, B., Mäkynen, M., Similä, M., Rontu, L., and Vihma, T.: Modelling snow and ice thickness in the coastal Kara Sea, Russia Arctic, Ann. Glaciol., 54(62), doi:10.3189/2013AoG62A180, 2013.

Comiso, J. C., Parkinson, L., Gersten, R., and Stock, L.: Accelerated decline in the Arctic sea ice cover, Geophys. Res.Lett., 35, L01703, doi10.1029/2007GL031972, 2008.

Dahlke, S., and Maturilli, M.: Contribution of Atmospheric Advection to the Amplified Winter Warming in the Arctic North Atlantic Region, Advances in Meteorol., doi:10.1155/2017/4928620, 2017.

Decker, M., Brunke, M. A., Wang, Z., Sakguchi, K., Zeng, X., and Bosilovich, M. G.: Evaluation of the reanalysis products from GSFC, NCEP, and ECMWF using flux tower observations, J. Clim., 25, 1916-1944, doi:10.1175/JCLI-D-11-00004.1, 2012.

Dee, D. P., Uppala, S. M., Simmons, A. J., Berrisford, P., Poli, P., Kobayashi, S., Andrae, U., Balmaseda, M. A., Balsamo, G., Bauer, P., Bechtold P., Beljaars, A. C. M., Berg, L. van de, Bidlot, J., Bormann, N., Delsol, C., Dragani, R., Fuentes, M., Geer, A. J., Haimberger, L., Healy, S. B., Hersbach, H., Hólm, E. V., Isaksen, L., Kållberg, P., Köhler, M., Matricardi, M., McNally, A. P., Monge-Sanz, B. M., Morcrette, J.-J., Park, B.-K., Peubey, C., Rosany, P. de, Tavolato, C., Thépaut, J.-N., and Vitart, F.: The ERA-Interim reanalysis: configuration and performance of the data assimilation system, Quart. J. Roy. Meteor. Soc., 137, 553-597, 2011.

Dutra, E., Schär, C., Viterbo, P., and Miranda, P. M. A.: Land-atmosphere coupling associated with snow cover, Geophys. Res. Lett., 38, L15707, doi:10.1029/2011GL048435, 2011.

Graham, R. M., Cohen, L., Petty, A. A., Boisvert, L. N., Rinke, A., Hudson, S. R., Nicolaus, M., and Granskog, M. A.: Increasing frequency and duration of Arctic winter warming events, Geophys. Res. Lett., 44, 6974-6983, doi:10.1002/2017GL073395, 2017a.

Graham, R. M., Rinke, A., Cohen, L., Hudson, S. R., Walden, V. P., Granskog, M. A., Dorn, W., Kayser, M., and Maturilli, M.: A comparison of the two Arctic atmospheric winter states observed during N-ICE2015 and SHEBA, J. Geophys. Res., Atmos., 122, 5716-5737, doi:10.1002/2016JD025475, 2017b.

Granskog, M. A., Rösel, A., Dodd, P. A., Divine, D., Gerland, S., Martma, T., and Leng, M. J.: Snow contribution to first-year and second-year Arctic sea ice mass balance north of Svalbard, J. Geophys. Res., Oceans, 122, 2539-2549, doi:10.1002/2016JC012398, 2017.

Graversen, R. G., Mauritsen, T., Tjernström, M., Källén, E., and Svensson, G.: Vertical structure of recent Arctic warming, Nature, 451(7174), 53-56, doi:10.1038/nature06502, 2008.

Grosfeld, K. Treffeisen, R., Asseng, J., Bartsch, A., Bräuer, B., Fritzsch, B., Gerdes, R., Hendricks, S., Hiller, W., Heygster, G., Krumpen, T., Lemke, P., Melsheimer, C., Nicolaus, M., Ricker, R., and Weigelt, M.: Online sea-ice knowledge and data platform <www.meereisportal.de>, Polarforschung, Bremerhaven, Alfred Wegener Institute for Polar and Marine Research and German Society of Polar Research, 85(22), 143-155, doi:10.2312/polfor.2016.011, 2016.

Huntermann, M., Heygster, G., Kaleschke, L., Krumpen, T., Mäkynen, M., and Drusch, M.: Empirical sea ice thickness retrieval during the freeze-up period from SMOS high incident angle observations, TC, 8, 439-451, doi:10.5194/tc-8-439-2014.

IFS documentation-CY41R2, Operational implementation, European Centre for Medium-Range Weather Forecasts, Shinfield Park, Reading, RG29AX, England, pp213, https://www.ecmwf.int/sites/default/files/elibrary/2016/16648-part-iv-physical-processes.pdf, 2016.

Jakobson, E., Vihma, T., Palo, T., Jakobson, L., Keernik, H., and Jaagus, J.: Validation of atmospheric reanalyses over the central Arctic Ocean, Geophys. Res. Lett., 39(10), L10802, doi:10.1029/2012GL051591, 2012.

Kapsch, M. L., Graversen, R. G., Economou, T., and Tjernström, M.: The importance of spring atmospheric conditions for predictions of the Arctic summer sea ice extent, Geophys. Res. Lett., 41, 5288–5296, doi:10.1002/2014GL060826, 2014.

Kayser, M., Maturilli, M., Graham, R. M., Hudson, S. R., Rinke, A., Cohen, L., Kim, J.-H., Park, S.-J., Moon, W., Granskog, M. A.: Vertical thermodynamic structure of the troposphere during the Norwegian young sea ICE expedition (N-ICE2015), J. Geophys. Res., Atmosphere, 122(20), doi:10.1002/2016JD026089, 2017.

King, J., Spreen, G., Gerland, S., Haas, C., Hendriks, S., Kaleschke, L., and Wang, C.: Sea-ice thickness from field measurements in the northwestern Barents Sea, J. Geophys. Res. Oceans, 122, 1497-1512, doi:10.1002/2016J012199, 2018.

Hersbach, H., and Dee., D: ERA5 reanalysis is in production, ECMWF Newsletter 147, ECMWF, http://ww.ecmwf.inten/elibrary/16299-newsletter-nol47-spring%g-2016 (last access: 24 March 2017), 2016.

Launiainen, J., and Cheng, B.: Modelling of ice thermodynamics in natural water bodies, Cold Reg. Sci. Technol., 27, 153-178, 1998.

Leeuw, J. De., Methven, J., and Blackburn, M.: Evaluation of ERA-Interim reanalysis precipitation products using England and Wales observations, Q. J. R. Meteorol. Soc., 141: 798-806, 2015, doi:10.1002/qi.2395, 2015.

Lei., R., Cheng, B., Heil, P., Vihma, T., Wang, J., Ji, Q., and Zhang, Z.: Seasonal and interannual variations of sea ice mass balance from the Central Arctic to the Greenland Sea, J. Geophys. Res.: Oceans, 123, 2422-2439, https://doi.org/10.1002/2017JC013548, 2017.

Leppäranta, M.: A growth model for black ice, snow ice and snow thickness in subarctic basins, Hydro. Res., 14(2), 59-70, 1978.

Lindsay, R., and Schweiger, A.: Arctic sea ice thickness loss determined using subsurface, aircraft, and satellite observations. TC, 9(1), 269–283, doi:10.5194/tc-9-269-2015, 2015.

Lindsay, R., Wensnahan, M., Schweiger, A., and Zhang, J.: Evaluation of seven different atmospheric reanalysis products in the Arctic, J. Clim., 27(7), 2588–2606, doi:10.1175/JCLI-D-13-00014, 2014.

Liston, G. E., Polashenski, C., Rösel, A., Itkin, P., King, J., Merkouriadi, I., and Haapala, J.,: A distributed snow-evolution model for sea-ice applications (SnowModel), J. Geophys. Res., Oceans, 123, 3786-3810. https://doi.org/10.1002/2017JC013706, 2018.

Lüpkes, C., Vihma, T., Jakobson, E., König-Langlo, G., and Tetzlaff, A.: Meteorological observations from ship cruises during summer to the central Arctic: A comparison with reanalysis data, Geophys. Res. Lett., 37(9), 850, doi:10.1029/2010GL042724, 2010.

Makshtas, A., Atkinson, D., Kulakov, M., Shutilin, S., Krishfield, R., and Proshutinsky, A.: Atmospheric forcing validation for modeling the central Arctic, Geophys. Res. Lett., 34, L20706, doi:10.1029/2007GL031378, 2007.

Maksimovich, E., and Vihma, T.: The effect of surface heat fluxes on interannual variability in the spring onset of snow melt in the central Arctic Ocean, J. Geophys. Res., 117, C07012, doi:10.1029/2011JC007220, 2012.

Markus, T., Stroeve, J. C., and Miller J.: Recent changes in Arctic sea ice melt onset, freezeup, and melt season length, J. Geophys. Res., 114, C12024, doi:10.1029/2009JC005436, 2009.

Maslanik, J., Stroeve, J., Fowler, C., and Emery, W.: Distribution and trends in Arctic sea ice age through spring 2011, Geophys. Res. Lett., 38, L13502, doi:10.1029/2011GL047735, 2011.

Maykut, G. A.: The surface heat and mass balance, in Geophysics of Sea Ice, edited by N. Untersteiner, pp. 395–463, Plenum, New York, 1986.

Meier, W. N., Fetterer, F., Savoie, M., Mallory, S., Duerr, R., and Stroeve, J.: NOAA/NSIDC climate data record of passive microwave sea ice concentration, Version 3. Boulder, Colorado USA, NSIDC: National Snow and Ice Data Center, doi:https://doi.org/10.7265/N59p2ZTG, 2017.

Merkouriadi, I., Cheng, B., Graham, R. M., Rösel, A., and Granskog, M. A.: Critical Role of Snow on Sea Ice Growth in the Atlantic Sector of the Arctic Ocean, Geophys. Res. Lett., 44(20), doi:10.1002/2017GL075494, 2017.

Mortin, J., Graversen, R. G., and Svensson, G.:. Evaluation of pan-Arctic melt-freeze onset in CMIP5 climate models and reanalyses using surface observations, Clim. Dyn., 42, 2239–2257, doi:10.1007/s00382-013-1811-z, 2014.

Mortin, J., Svensson, G., Graversen, R. G., Kapsch, M. L., Stroeve, J. C., and Boisvert, L. N.: Melt onset over Arctic sea ice controlled by atmospheric moisture transport, Geophys. Res. Lett., 43(12), 6636–6642, doi:10.1002/2016GL069330, 2016.

Nicolaus, M., Hoppmann, M., Arndt, S., Hendricks, S., Kaltein, C., König-Langlo, G., Nicolaus, A., Rossmann, L., Schiller, M., Schwegmann, S., Langevin, D., Bartsch, A.: Snow height and air temperature on sea ice from snow buoy measurements, Alfred Wegener Institute, Helmholtz Center for Polar and Marine Research, Bremerhaven, PANGAEA, doi:0.1594/PANGAEA.875638, 2017.

Olauson, J.: ERA5: The new champion of wind power modelling? Renew. Energy, 126, 322-331, doi.org/10.1016/j.renene.2018.03.056, 2018.

Perovich, D., Richter-Menge, J., and Polashenski, C.: Observing and understanding climate changes: Monitoring the mass balance, motion, and thickness of Arctic sea ice, http://imb.crrel-datmouth.org, 2018.

Polashenski, C., Perovich, D., Richter-Menge, J., and Elder, B.: Seasonal ice mass-balance buoys: adapting tools to the changing Arctic, Ann. Glaciol., 52(57), 18- 26, 2011.

~~Polyakov, I. V., Timokhov, L. A., Alexeev, V. A., Bacon, S., Dimtrenko, I. A., Fortier L, Frolov, I. E., Gascard, J.-C., Hansen, E., Ivanov, V. V., Laxon, S., Mauritzen, C., Perovich, D., Shimada, K., Simmons, H. L., Sokolov, V. T., Steele, M., and Toole, J.: Arctic ocean warming contributes to reduced polar ice cap, J. Phys. Oceanogr., 40, 2743-2756, 2010.~~

Rasmussen, R., Baker, B., Kochendorfer, J., Meyers, T., Landolt, S., Fischer, A. P., Black, J., Thériault, J. M., Kucera, P., Gochis, D., Smith, C., Nitu, R., Hall, M., Ikeda, K., and Gutmann, E.: How well are we measuring snow: The NOAA/FAA/NCAR winter precipitation test bed, Bull. Amer. Meteor. Soc., 93, 811- 829, doi: 10.1175/BAMS-D-11-00052.1, 2012.

Richter-Menge, J., Perovich, D. K., Elder, B. C., Claffey, K., Rigor, I., and Ortmeyer M.: Ice mass balance buoys: a tool for measuring and attributing changes in the thickness of the Arctic sea ice cover, Ann. Glaciol., 44, 205-210, 2006.

Rigor, I. G., Colony, R. L., and Martin, S.: Variations in Surface Air Temperature Observations in the Arctic, 1979 – 97, J. Clim., 13, 896–914, 2000.

Rinke, A., Maturilli, M., Graham, R. M., Matthes, H., Handorf, D., Cohen, L., Hudson, S. R., and Moore J. C.: Extreme cyclone events in the Arctic: Wintertime variability and trends, Environ. Res. Lett., 12(9), doi:10.1088/1748-9326/aa7def, 2017.

Sato, K., and Inoue, J.: Comparison of Arctic sea ice thickness and snow depth estimates from CFSR with in situ observations, Clim. Dyn., 50(1), 1–13, doi:10.1007/s00382-017-3607-z, 2017.

Schweiger, A., Lindsay, R., Zhang, J., Steele, M., Stern, H., and Kwok, R.: Uncertainty in modeled Arctic sea ice volume, J. Geophys. Res., Ocean, 116(9), 1–21, doi:10.1029/2011JC007084, 2011.

Screen, J. A., and Simmonds, I.: The central role of diminishing sea ice in recent Arctic temperature amplification, Nature, *464*(7293), 1334–1337, doi:10.1038/nature09051, 2010.

Sotiropoulou, G., Sedlar, J., Forbes, R., and Tjernström, M.: Summer Arctic clouds in the ECMWF forecast model: An evaluation of cloud parameterization schemes, Quart. J. Roy. Meteor. Soc., 142, 387-400, doi:10.1002/qj.2658, 2015.

~~Steel, M., Ermold, W., and Zhang, J.: Arctic ocean surface warming trends over the past 10 years, Geophys. Res. Lett., 35, L02614, doi:10.1029/98GL00251, 2008.~~

Stroeve, J., and Notz D.: Chaning state of Arctic sea ice across all the seasons, Env. Res. Lett., 13, 103001, https://doi.org/10.1088/1748-9326/aade56, 2018.

Stroeve, J. C., Serreze, M. C., Holland, M. M., Kay, J. E., Malanik, J., and Barrett A. P.: The Arctic's rapidly shrinking sea ice cover: A research synthesis, Clim. Change, 110(3-4), 1005–1027, doi:10.1007/s10584-011-0101-1, 2012.

Stroeve, J. C., Markus, T., Boisvert, L., Miller, J., and Barrett, A.: Changes in Arctic melt season and implications for sea ice loss, Geophys. Res. Lett., 41, 1216-1225, doi:10.1002/2013GL058951, 2014.

Stroeve, J., Schroder, D., Tsamados, M., and Feltham, D.: Warm Winter, Thin Ice? The Cryosphere, 1791–1809, doi:10.5194/tc-12-1791-2018, 2018.

Sturm, M., Holmgren, J., and Perovich, D. K.: Winter snow cover on the sea ice of the Arctic Ocean at the Surface Heat Budget of the Arctic Ocean (SHEBA): Temporal evolution and spatial variability, J. Geophys. Res., 107(C10), 8047, doi:10.1029/2000JC000400, 2002.

Tjernstöm, M., and Graversen, R. G: The Vertical Structure of the lower Arctic troposphere analysed from observations and the ERA-40 reanalysis, Quart. J. Roy. Meteor. Soc., 135, 431-443, doi:10.1002/qj.380, 2009.

Urraca, R., Huld, T., Gracia-Amillo, A., Martinez-de-Pison, F. J., Kaspar, F., and Sanz-Garcia, A.: Evaluation of global horizontal irradiance estimates from ERA5 and COSMO-REA6 reanalysis using ground and satellite-based data, Sol. Energy, 164, 339-354, doi.org/10.1016/j.solener.2018.02.059, 2018.

Vihma, T., Pirazzini, R., Fer, I., Renfrew, I. A., Sedlar, J., Tjernström, M., Lüpkes, C., Nygård, T., Notz, D., Weiss, J., Marsan, D., Cheng, B., Birnbaum, G., Gerland, S., Chechin, D., and Gascard, J. C..: Advances in understanding and parameterization of small-scale physical processes in the marine Arctic climate system: a review, Atmos. Chem. Phys., 14, 9403-9450, www.atmos-chem-phys.net/14/9403/2014/, doi:10.5194/acp-14-9403-2014, 2014.

Wang, C., Shi, L., Gerland, S., Granskog, M. A., Renner, A. H. H., Li, Z., Hansen, and Martma, T.: Spring sea-ice evolution in Rijpfjorden (80° N), Svalbard, from in-situ measurements and ice mass-balance buoy (IMB) data, Ann. Glacio., 54(62), doi:10.3189/2013AoG62A135, 2013.

Wang, C., Cheng, B., Wang, K., Gerland, S., and Pavlova O.: Modelling snow ice and superimposed ice on landfast sea ice in Kongsfjorden, Svalbard, Polar Res., 34, 20828, http://dx.doi.org/10.3402/polar.v34.20828, 2015.

Warren, S. G., Rigor, I. G., Untersteiner, N., Radionov, V. F., Bryazgin, N. N., Aleksandrov, Y. I., and Colony, R.: Snow depth on Arctic sea ice, J. Clim., 12, 1814-1829, 1999.

Webster, M., Gerland, S., Holland, M., Hunke, E., Kwok, R., Lecomte, O., Massom, R., Perovich, D., and Sturm, M.: Snow in the changing sea-ice systems, Nat. Clim. Change, doi.org/10.1038/s41558-018-0286-7, 2018.

Wesslén, C., Tjernström, M., Bromwich, D. H., De Boer, G., Ekman, A. M. L., Bai, L. S., and Wang, S. H.: The Arctic summer atmosphere: An evaluation of reanalyses using ASCOS data, Atmos. Chem. Phys., 14(5), 2605–2624, doi:10.5194/acp-14-2605-2014, 2014.

Woods, C., and Caballero R.: The role of moist intrusions in winter Arctic warming and sea ice decline, J. Clim., 29, 4473-4485, doi:10.1175/JCLI-D-15-0773.1, 2016.

Table 1. Summary of deployment locations and initial conditions for the buoys. The accumulated snow water equivalent (SWE) is given based on ERA-I, ERA5 and buoy data. The cumulative SWE ~~solid precipitation (Sp)~~TP is based on total precipitation assuming precipitation falls as snow when T2M is <0 °C. The cumulative snowfall (~~Sf~~SF) is calculated in the same period as what did for the cumulative ~~Sp~~TP. The accumulated SWE measured by the buoy is estimated using ~~assuming~~ a climatological monthly mean snow density ~~of 350 kg m-3~~based on Warren et al. (1999).

Buoy	Deployment location	Period of operation	Ice type	Initial thickness (m)		Accumulated SWE (mm water equivalent)				
						ERA-I		ERA5		Buoy
				ice	snow	~~Sp~~TP	~~Sf~~SF	~~Sp~~TP	~~Sf~~SF	SWE
2010A	Central Arctic	20 Apr 2010 – 2 Dec 2010	FYI	1.67	0.24	77.5[B]	51.8[B]	71.8[B]	70.7[B]	~~84.0~~67.2[B]
2011M	Central Arctic	29 Sept 2011 – 22 Apr 2013	MYI	1.67	0.07	94.6[A]	89.2[A]	56.2[A]	56.2[A]	~~56.0~~19.2[A]
2012C	Central Arctic	13 Apr 2012 - 4 Oct 2012	FYI	1.24	0.43	56.2[B]	21.1[B]	26.2[B]	22.9[B]	NA
2012D	Central Arctic	4 May 2012 - 2 Nov 2012	FYI	1.67	0.47	89.9[B]	47.1[B]	86.9[B]	77.3[B]	~~161.0~~124.2[A]
2012H	Beaufort Sea	10 Sept 2012 - 16 Jan 2014	FYI	1.50	0.02	75.8[A]	68.1[A]	46.7[A]	46.7[A]	~~70~~63.0[A]
2012L	Beaufort Sea	27 Aug 2012 - 25 Sept 2013	MYI	3.35	0.02	76.9[A]	69.3[A]	57.8[A]	57.7[A]	1~~4.0~~2.8[A]
2012I	Chukchi Sea	14 Aug 2012 - 21 Dec 2012	MYI	1.09	0.10	94.8[B]	71.1[B]	85.7[B]	80.0[B]	~~119~~98.0[B]
2012J	Laptev Sea	25 Aug 2012 – 11 Jan 2014	MYI	1.09	0	80.3[A]	71.2[A]	60.5[A]	60.5[A]	~~52.5~~41.6[A]
2013B	Central Arctic	10 Apr 2013 - 19 Dec 2013	NA	2.00	0.02	151.3[B]	104.0[B]	135.5[B]	117.5[B]	~~84.0~~36.4[B]
2013E	Central Arctic	11 Apr 2013 - 4 Oct 2013	FYI	1.40	0.05	57.4[B]	17.8[B]	37.7	35.1[B]	NA
2013H	Central Arctic	3 Sept 2013 - 29 Dec 2013	NA	1.30	0.05	42.3[C]	38.3[C]	34.7[C]	34.7[C]	~~17.5~~20.3[C]
2014E	Central Arctic	11 Apr 2014 - 18 Feb 2015	NA	1.73	0.19	182.6[B]	122.9[B]	156.1[B]	145.7[B]	1~~40.0~~03.6[B]
2015D	Central Arctic	10 Apr 2015 - 1 Feb 2016	NA	1.96	0.05	144.4[C]	110.7[C]	140.2[C]	136.7[C]	~~392~~354.0[C]
s16	Laptev Sea	19 Sept 2015 - 20 Dec 2016	FYI	NA	0.07	123.6[A]	107.6[A]	105.8[A]	105.8[A]	~~91~~80.0[A]
s20	Central Arctic	14 Sept 2015 – 19 Apr 2016	FYI	1.50	0.05	84.0[C]	76.8[C]	54.3[C]	54.2[C]	~63~~35~~.0[C]
s29	Laptev Sea	10 Sept 2015 - 16 Oct 2016	FYI	1.20	0.01	108.5[A]	95.9[A]	85.0[A]	84.9[A]	~~70~~20.0[A]

NA: no data

[A]: from 1 October to 30 April.

[B]: from 15 August until the IMB fails or there is no snow data.

[C]: from 1 October until the buoy fails or there is no longer snow data during the first freezing season

Table 2. The mean T2M, accumulated FDD, and estimated ice growth with FDD model

Buoy	T2M mean (°C)			FDD (K·d)[A] /ice growth (m)[B]		
	ERA5	ERA-I	Buoy	ERA5	ERA-I	Buoy
2011M	-22.5	-24.2	-26.6	4295/1.70	4662/1.78	5174/1.90
2012H	-22.5	-24.1	-25.8	4276/1.70	4624/1.78	4978/1.85
2012L	-22.1	-23.1	-24.9	4198/1.68	4402/1.73	4788/1.81
2012J	-20.8	-20.8	NA	~~4198~~3902/1.~~68~~61	~~4402~~3921/1.~~72~~61	NA

NA: no data

[A]: from 1 October to 30 April.

[B]: ice growth estimation by the end of freezing season with the Lebedev FDD model (Maykut, 1986).

Table 3. Model runs and ~~A~~atmospheric forcing data in model simulations, where TP is total precipitation, SF is snowfall, ~~U10~~ V is wind at 10 m height ~~(U10)~~, Rh is relative humidity ~~(Rh)~~, and ~~Tcc~~ CN is total cloud cover ~~(Tcc)~~.

Model runs	T2M	Precipitation	~~U10~~V, Rh, ~~Tcc~~CN
~~Sp-ERA~~TPI_T2MI	ERA-I	~~Sp~~ TP from ERA-I	ERA-I
~~Sp-ERA~~TP5_T2M5	ERA5	~~Sp~~ TP from ERA5	ERA5
S~~f_ERAI~~FI_T2MI	ERA-I	~~Sf~~ SF from ERA-I	ERA-I
S~~f_ERA5~~F5_T2M5	ERA5	~~Sf~~ SF from ERA5	ERA5
~~T2M-ERA5_Sp-ERA~~TPI_T2M5	ERA5	~~Sp~~ TP from ERA-I	ERA-I
~~T2M-ERAI_Sp-ERA~~TP5_T2MI	ERA-I	~~Sp~~ TP from ERA5	ERA-I

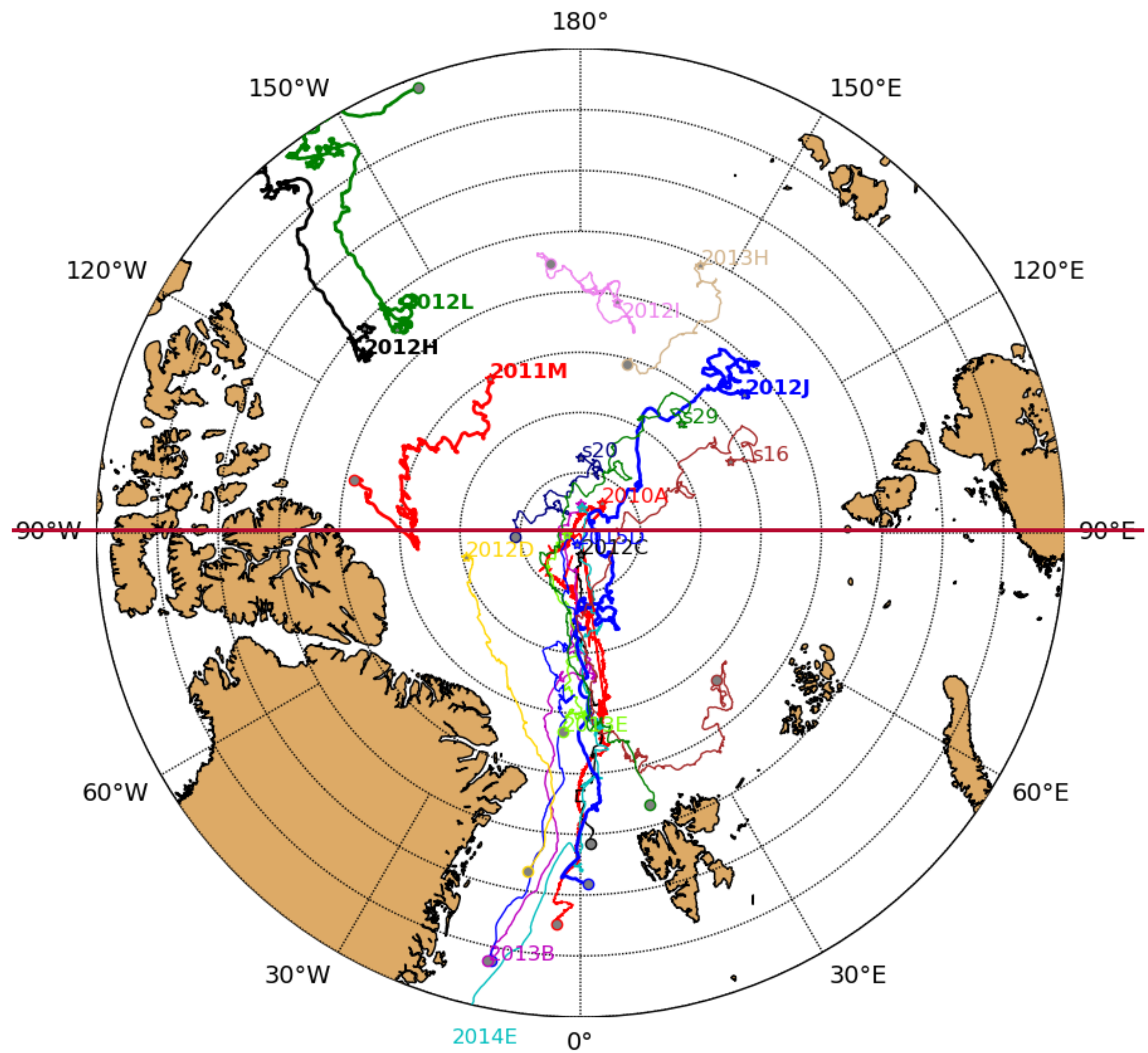

180°
150°W
150°E
120°W
120°E
90°W
90°E
60°W
60°E
30°W
30°E
0°
2013H
2012I
2012L
2012H
2011M
2012J
s29
s16
s20
2010A
2012C
2012D
2013E
2013B
2014E

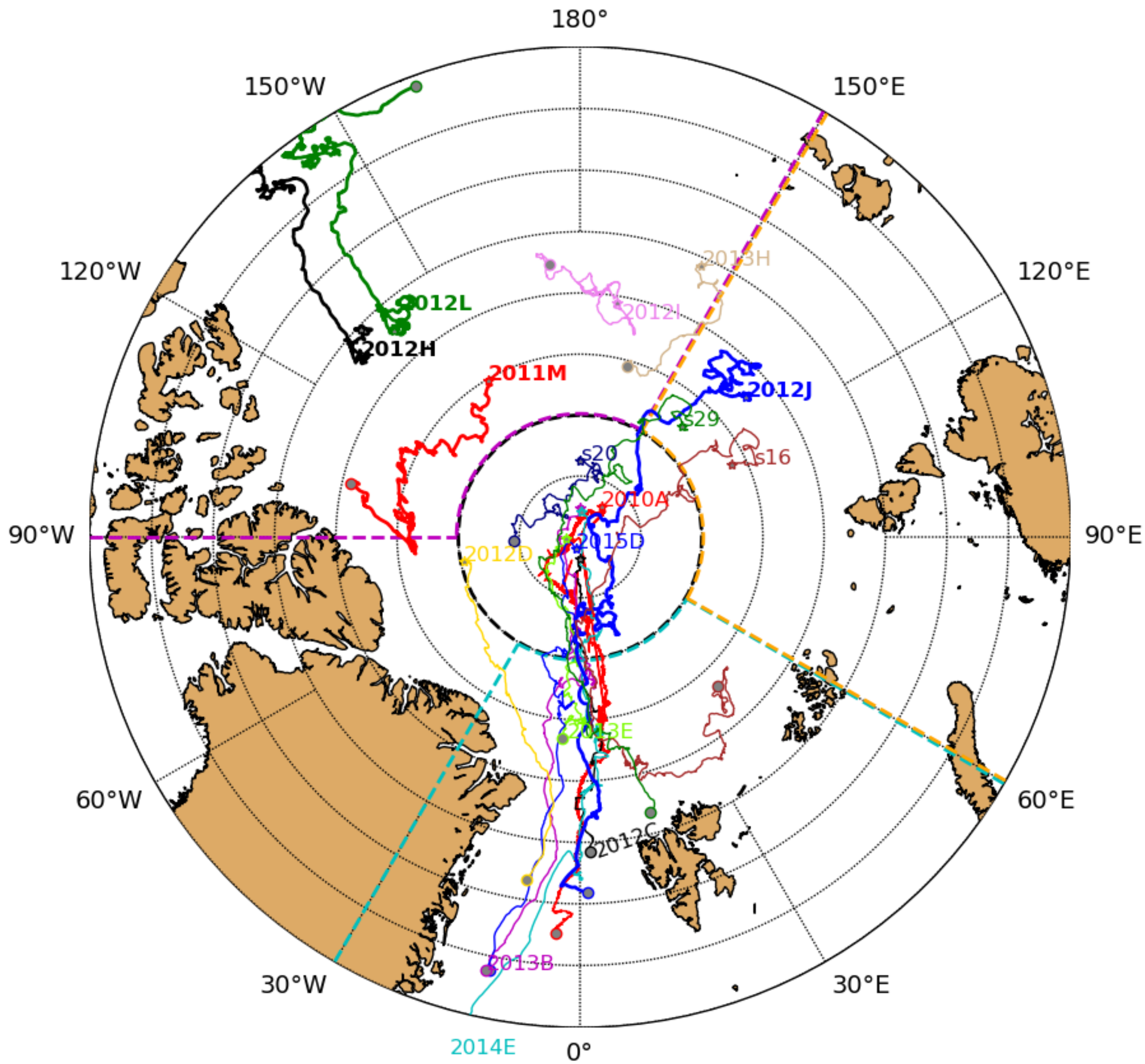

Figure 1. Drift trajectories of all ~~the~~ selected buoys (IMBs and snow buoys). Symbol "⋆" indicates the start of the drift and "o" signals the end of the drift. Buoys' names are labelled at the beginning or the end of the drift using same colour as lines. Buoys used for model simulations are highlighted with solid thick line and bold font. <u>Dashed thick lines illustrate our definition for sectors: Central Arctic (black; north of 86° N), and south of 86°N: Pacific sector (magenta; 90° W-150° E), Atlantic sector (cyan; 30° W–60° E) and Laptev Sea (orange; 60° E – 150° E) used in Figure 6.</u>

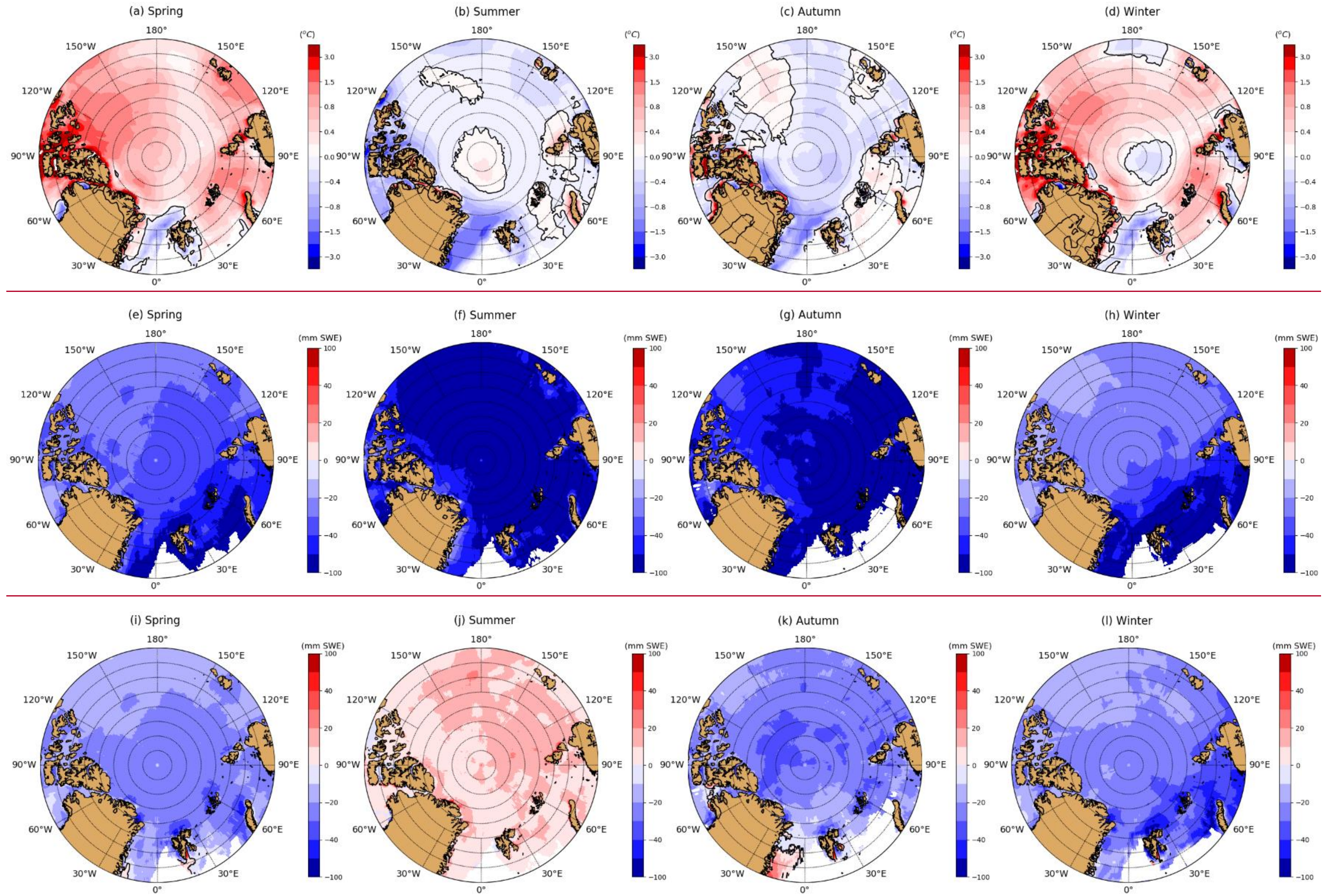

Figure 2. Seasonal mean difference between ERA5 and ERA-I (ERA5-ERA-I) for T2M (a-d), total precipitation (e-h), and snowfall (i-l) in spring (a, e, i), summer (b, f, j), autumn (c, g, k) and winter (d, h, l) over Arctic sea ice during 2010-2015. The sea ice extent is seasonal mean during the same period.

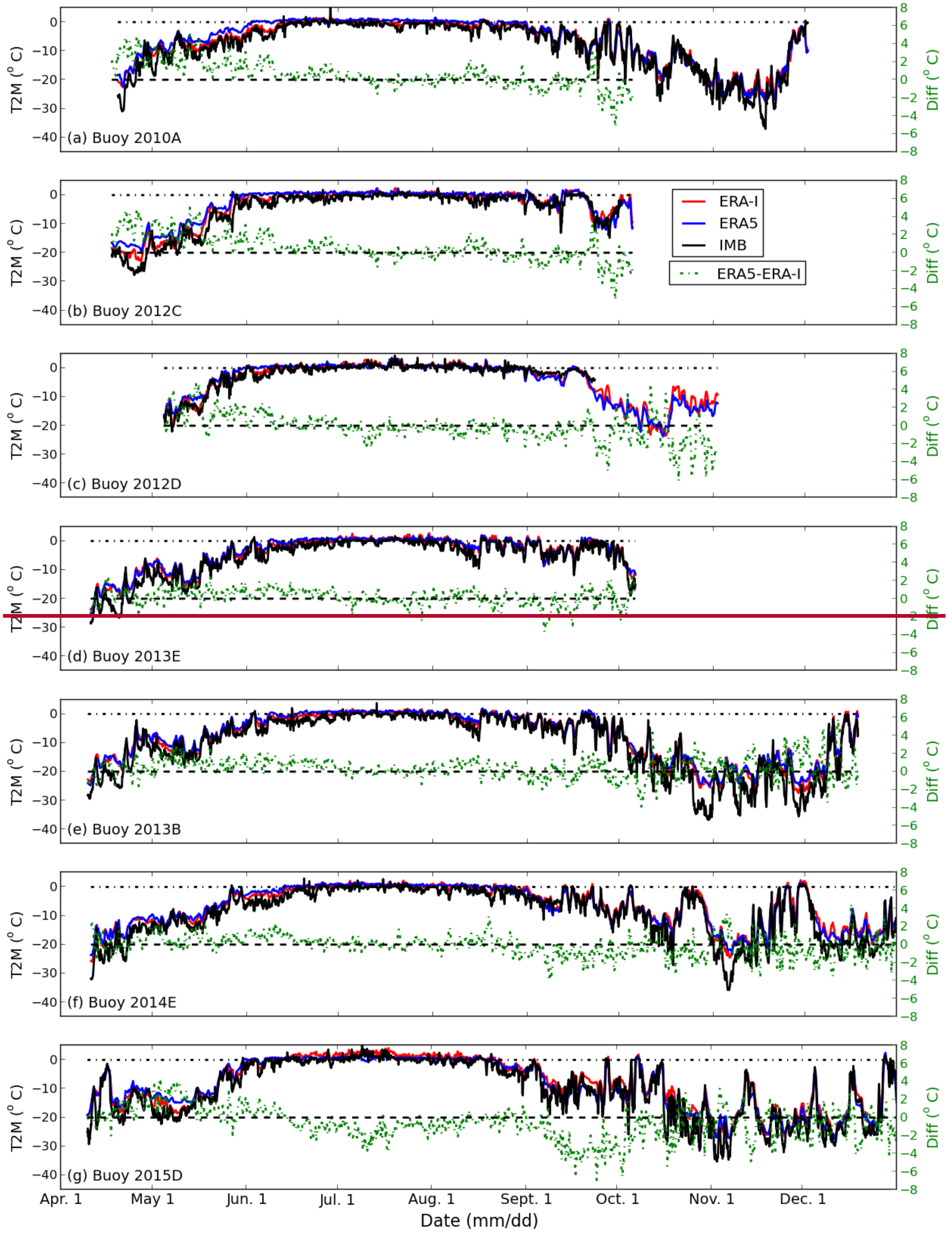

(a) Buoy 2010A
(b) Buoy 2012C
(c) Buoy 2012D
(d) Buoy 2013E
(e) Buoy 2013B
(f) Buoy 2014E
(g) Buoy 2015D
ERA-I
ERA5
IMB
ERA5-ERA-I
T2M (° C)
Diff (° C)
Apr. 1
May 1
Jun. 1
Jul. 1
Aug. 1
Sept. 1
Oct. 1
Nov. 1
Dec. 1
Date (mm/dd)

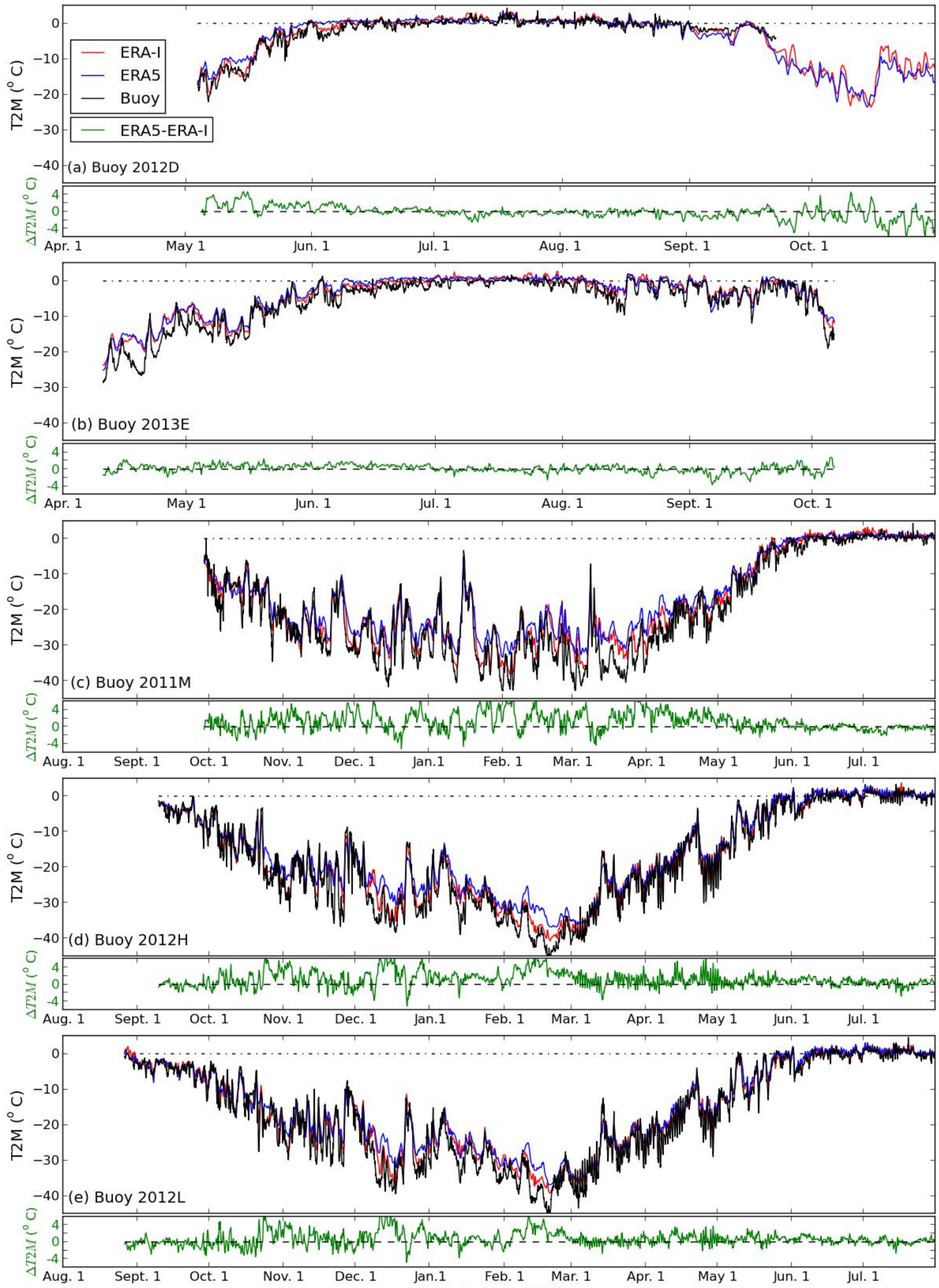

Figure 3~~2~~. Variation of 2 m air temperature (T2M) in ERA5, ERA-I and the buoys ~~(left side y-axis)~~ and the differences of T2M between ERA5 and ERA-I ~~(right side green y-axis)~~ for buoys (a) 2012D, (b) 2013E, (c) 2011M, (d) 2012H, and (e) 2012L~~deployed in April~~. Note the different time-axis.

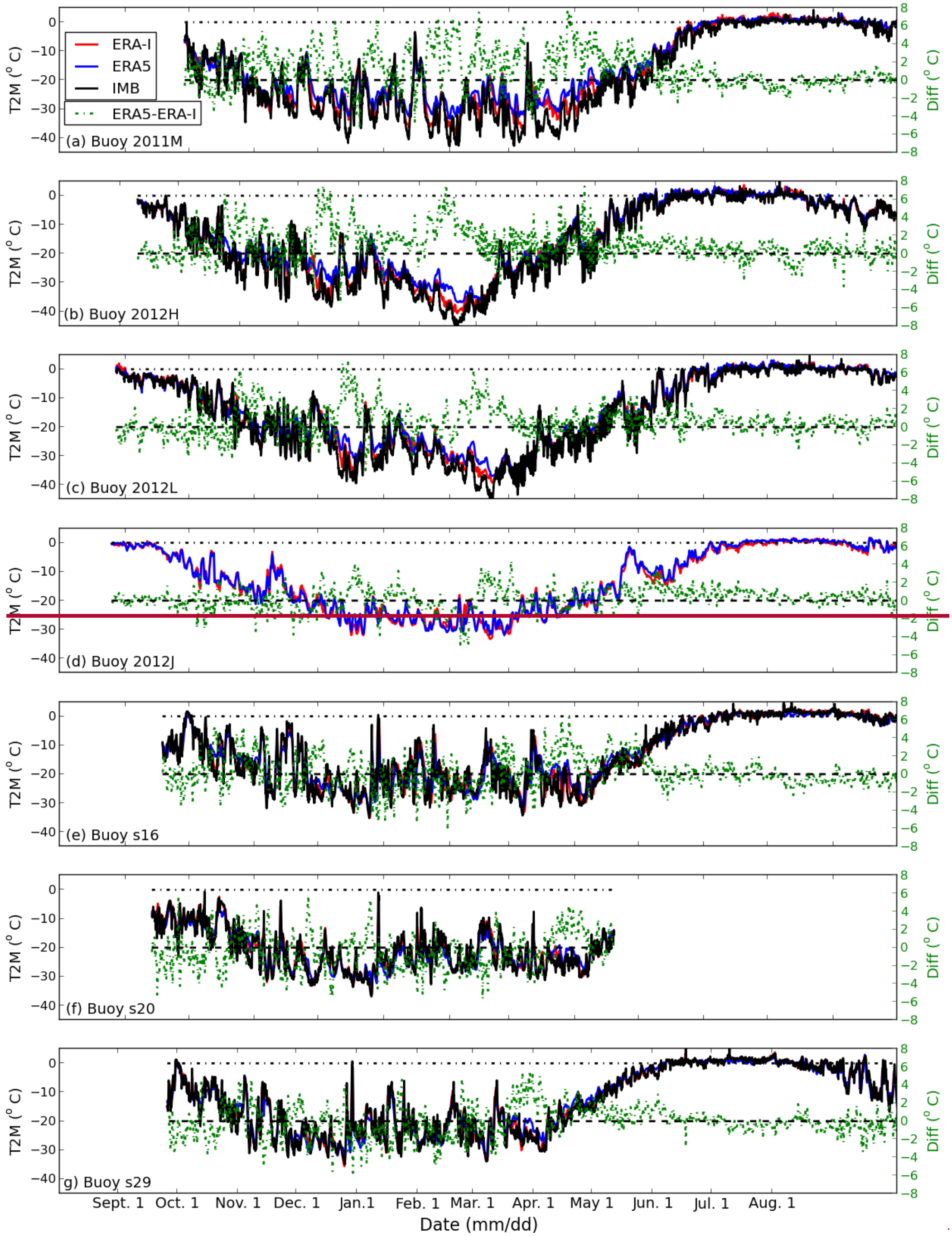
ERA-I
ERA5
IMB
ERA5-ERA-I
(a) Buoy 2011M
(b) Buoy 2012H
(c) Buoy 2012L
(d) Buoy 2012J
(e) Buoy s16
(f) Buoy s20
g) Buoy s29
T2M (° C)
Diff (° C)
Sept. 1
Oct. 1
Nov. 1
Dec. 1
Jan.1
Feb. 1
Mar. 1
Apr. 1
May 1
Jun. 1
Jul. 1
Aug. 1
Date (mm/dd)

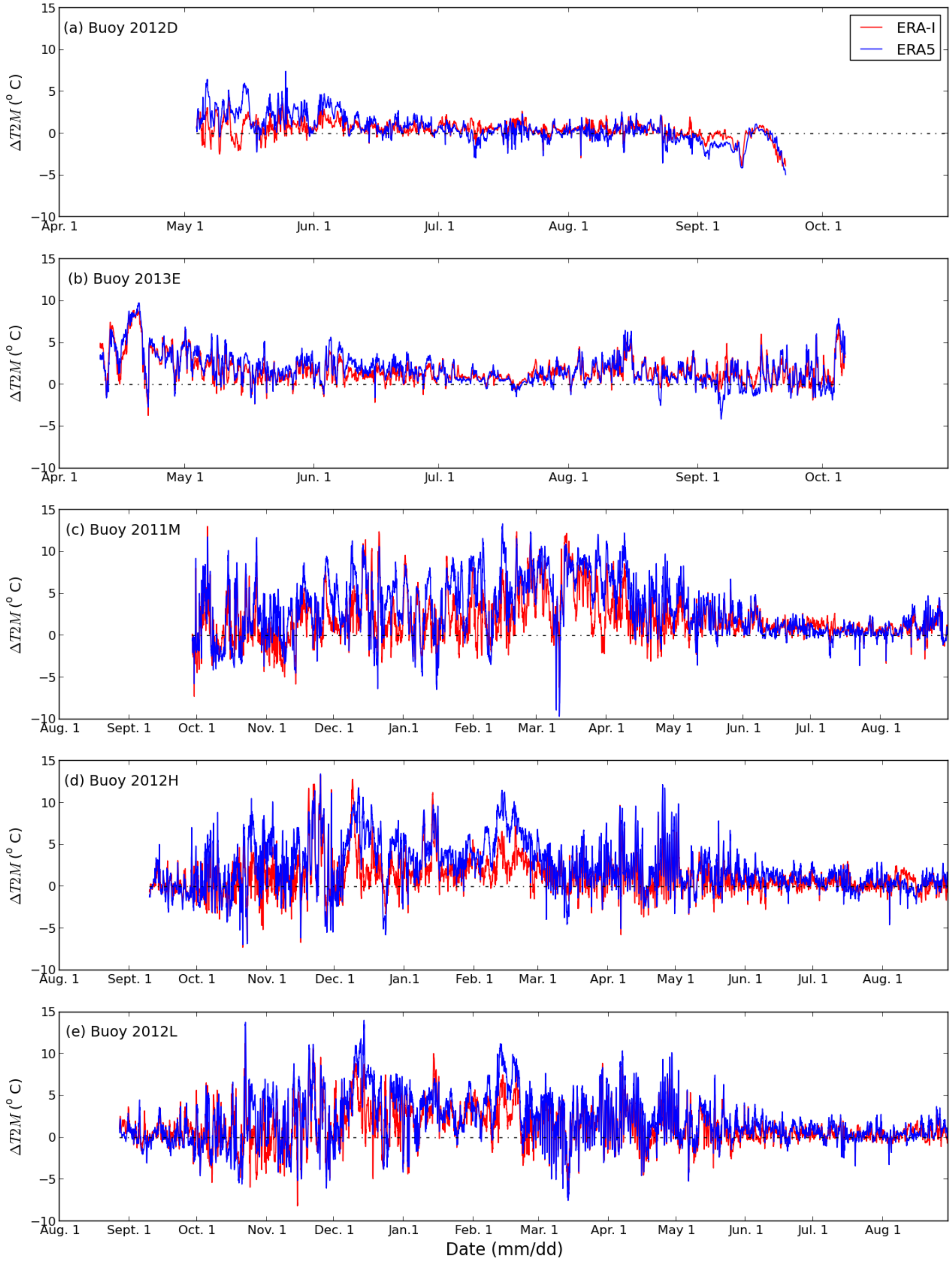

Figure ~~3~~4. ~~Same as Figure 2, but for buoys deployed from September-October. There is no black line in panel (k) due to no observational data.~~Variation of T2M differences between ERA5/ERA-I and buoys for (a) buoy 2012D, (b) buoy 2013E, (d) buoy 2011M, (d) buoy 2012H, and (e) buoy 2012L.

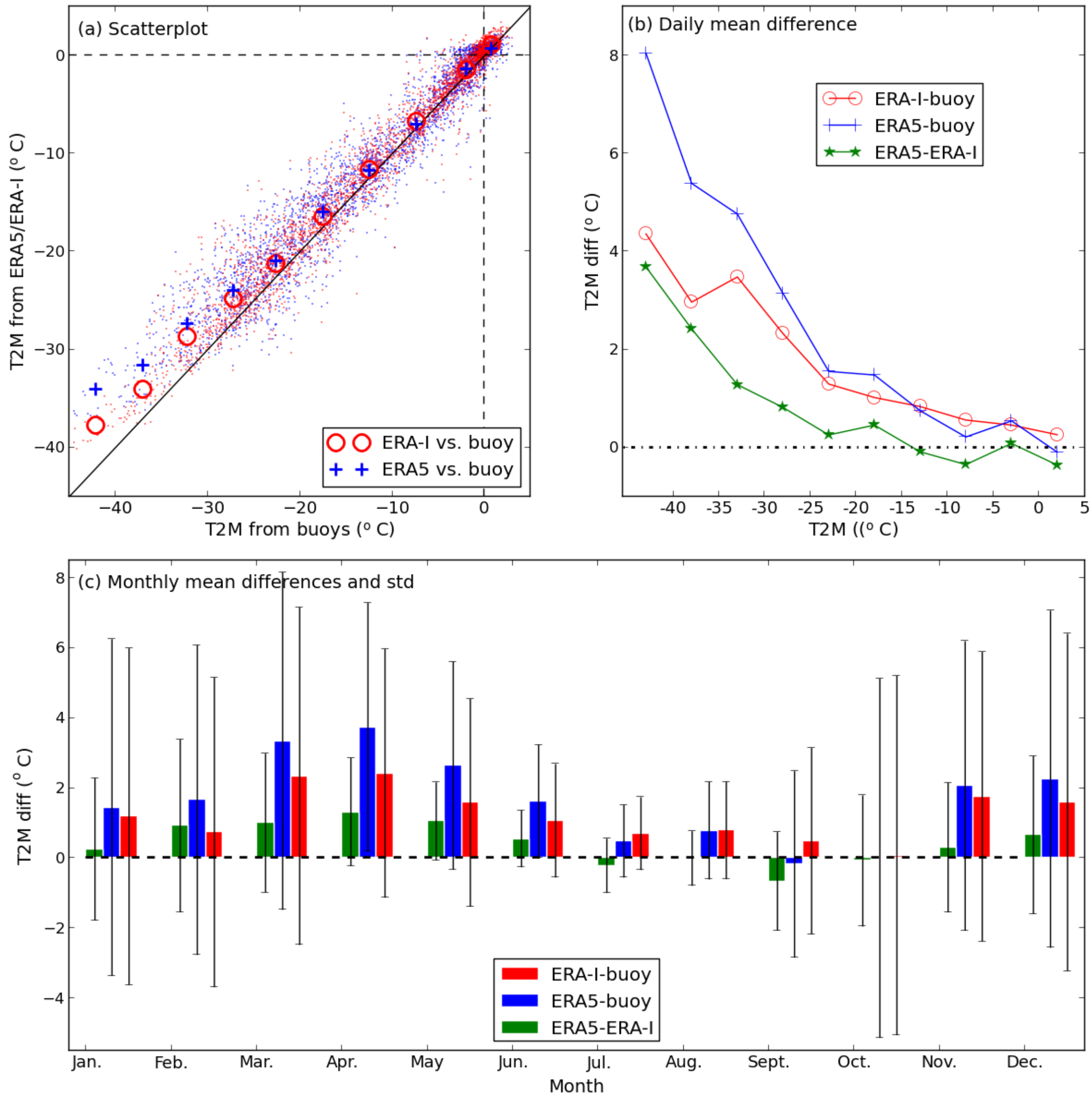

Fig. ~~4~~5. Statistics of T2M from ERA5, ERA-I and all the buoys. (a) Scatter plot for all data (small dots) and average T2M at 5 degree bins between -45 °C and +5 °C, (b) Daily temperature differences between the reanalysis and between the reanalysis and the buoys corresponding to 5 degree bins between -45 °C and +5 °C, and (c) monthly mean differences and standard deviation (std). In panel a, the black solid line is for 1:1.

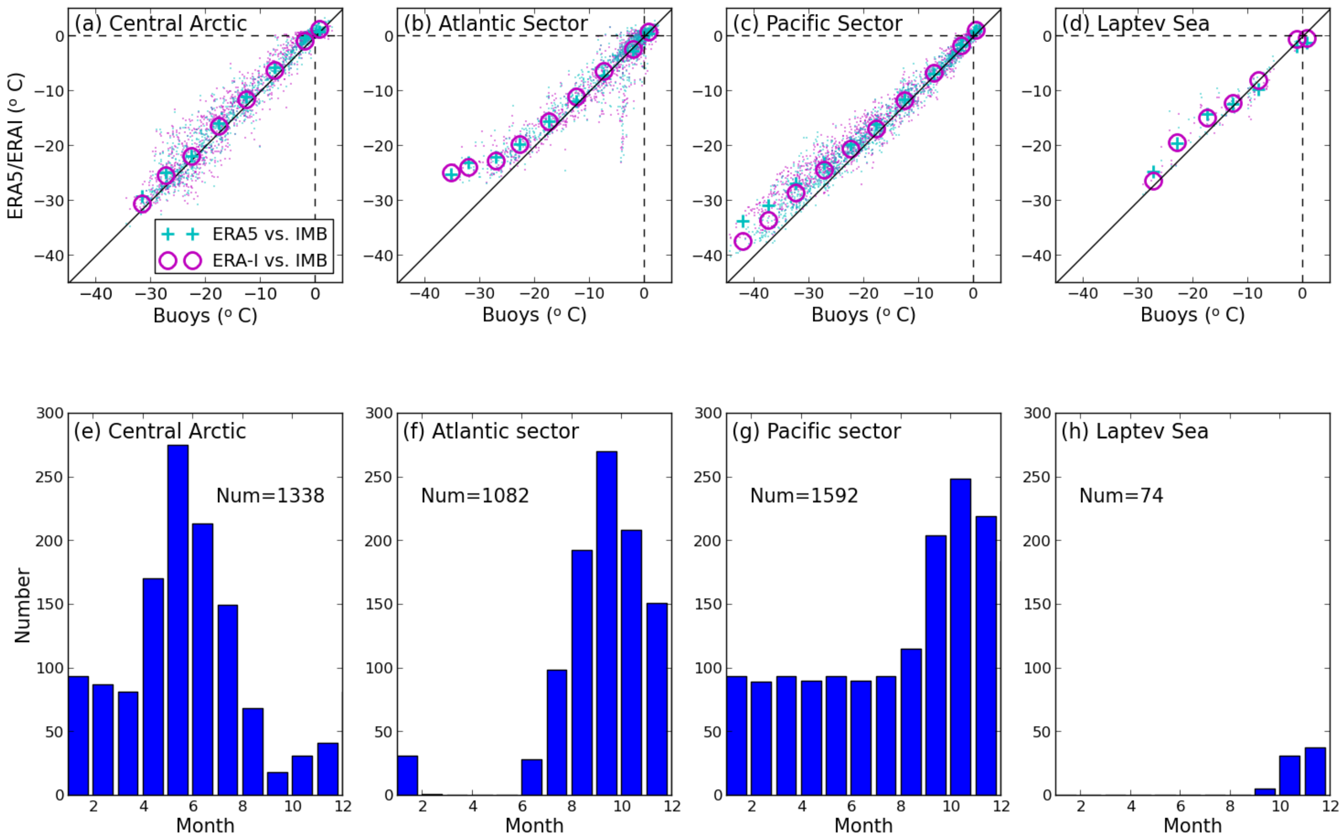

Figure 6. Scatter plot of T2M from ERA5 and ERA-I vs. from buoys for (a) Central Arctic, (b) Atlantic sector, (c) Pacific sector, and (d) Laptev Sea, and number of buoy data (daily) per month for (e) Central Arctic (f) Atlantic sector, (g) Pacific sector, and (h) Laptev sea. The definition of sectors are shown in Figure 1.

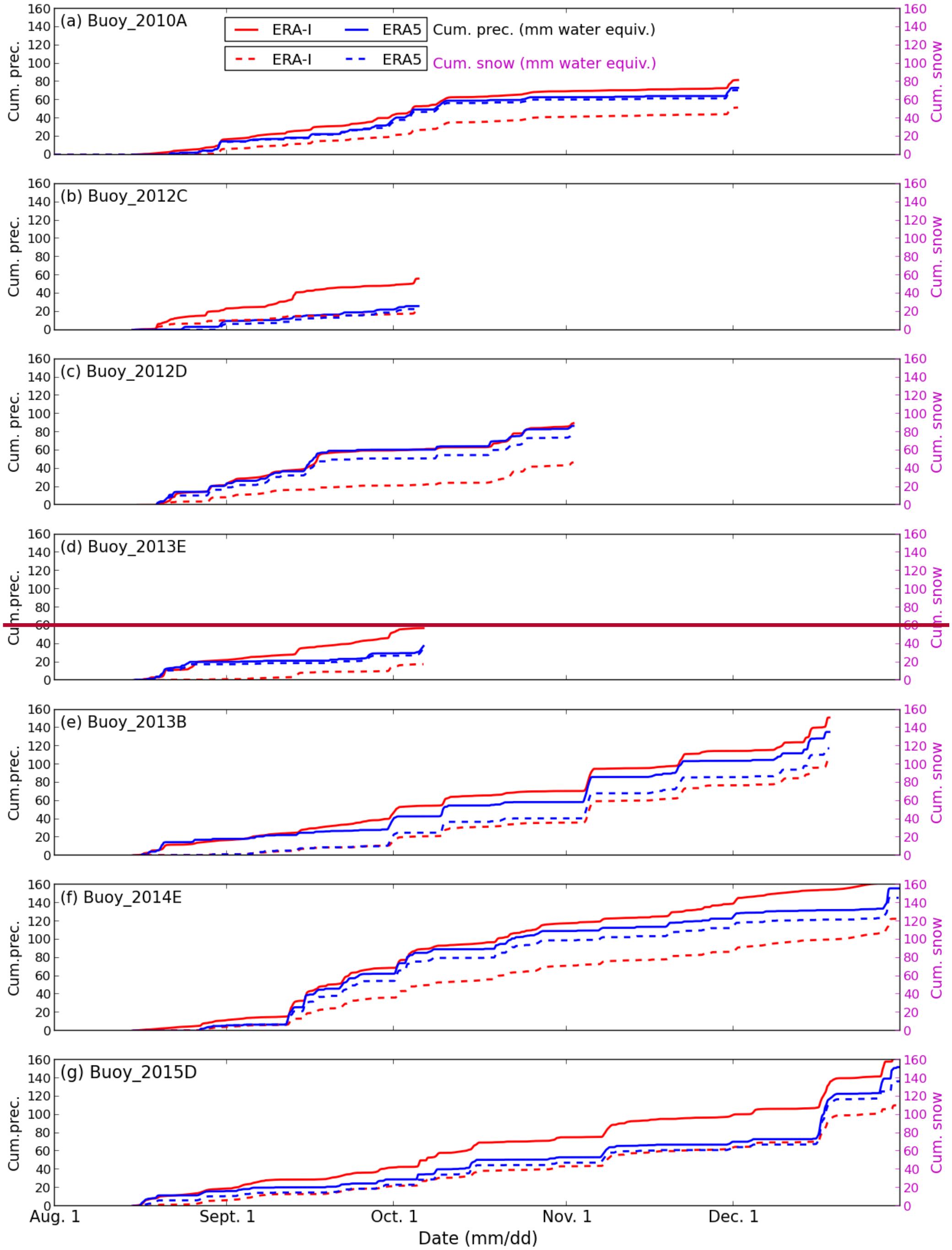
(a) Buoy_2010A
(b) Buoy_2012C
(c) Buoy_2012D
(d) Buoy_2013E
(e) Buoy_2013B
(f) Buoy_2014E
(g) Buoy_2015D
ERA-I
ERA5
Cum. prec. (mm water equiv.)
Cum. snow (mm water equiv.)
Cum. prec.
Cum. snow
Aug. 1
Sept. 1
Oct. 1
Nov. 1
Dec. 1
Date (mm/dd)

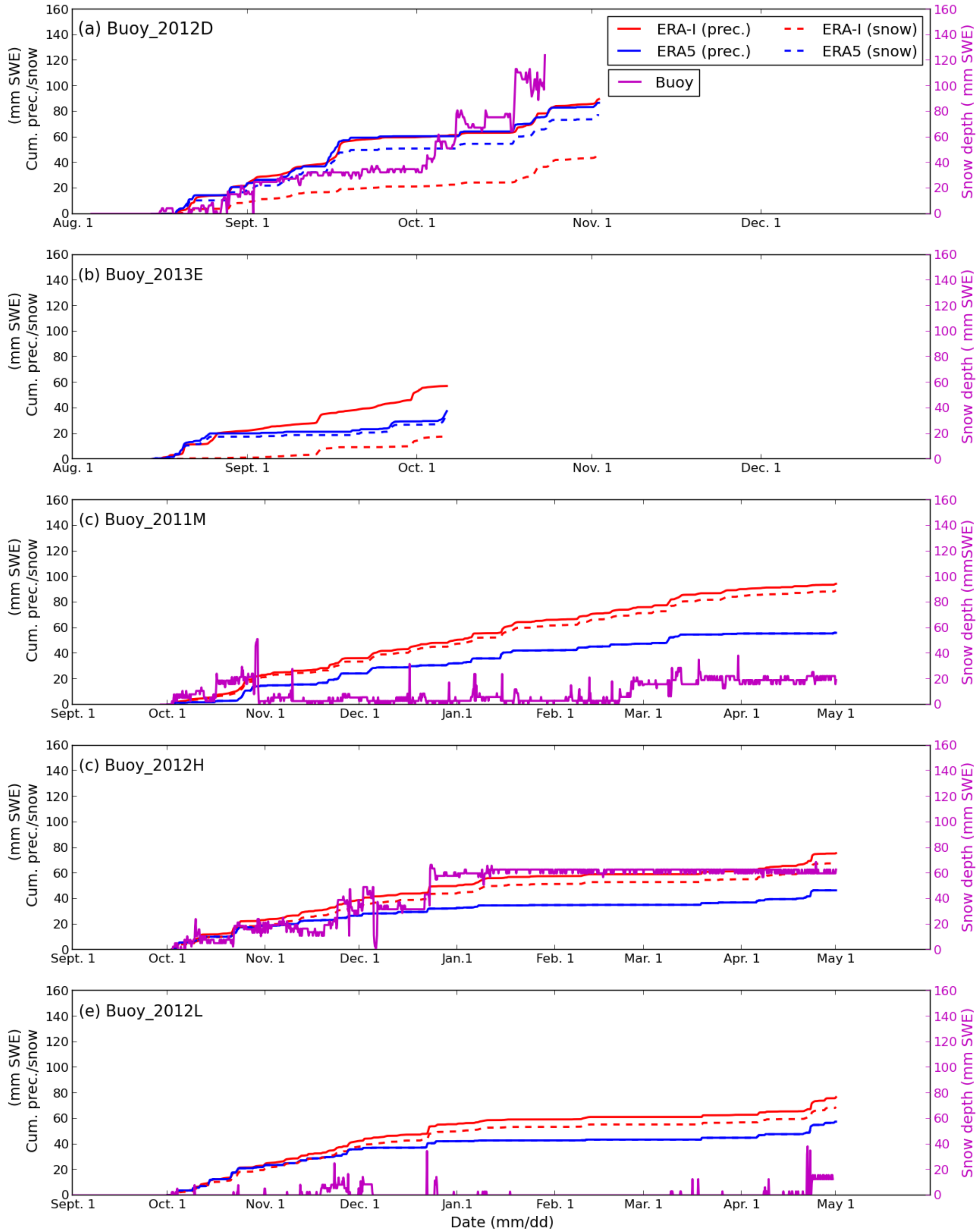

Figure 7~~5~~. Cumulative total precipitation (~~left side y-axis~~prec.) and snowfall (~~right side magenta y-axis~~snow) for ERA5 and ERA-I and snow depth for buoys (a) 2012D, (b) 2013E, (c) 2011M, (d) 2012H, and (e) 2012L. ~~with a~~Accumulation ~~starting~~ starts from 15 August for panels (a) and (b), and~~. Red lines are for ERA-I, and blue lines are for ERA5, with solid lines for the cumulative total~~

~~precipitation, and dashed lines for the cumulative snowfall~~ from 1 October for panels (c)-(e). Note there was no snow depth data for buoy 2013E during the accumulation period.

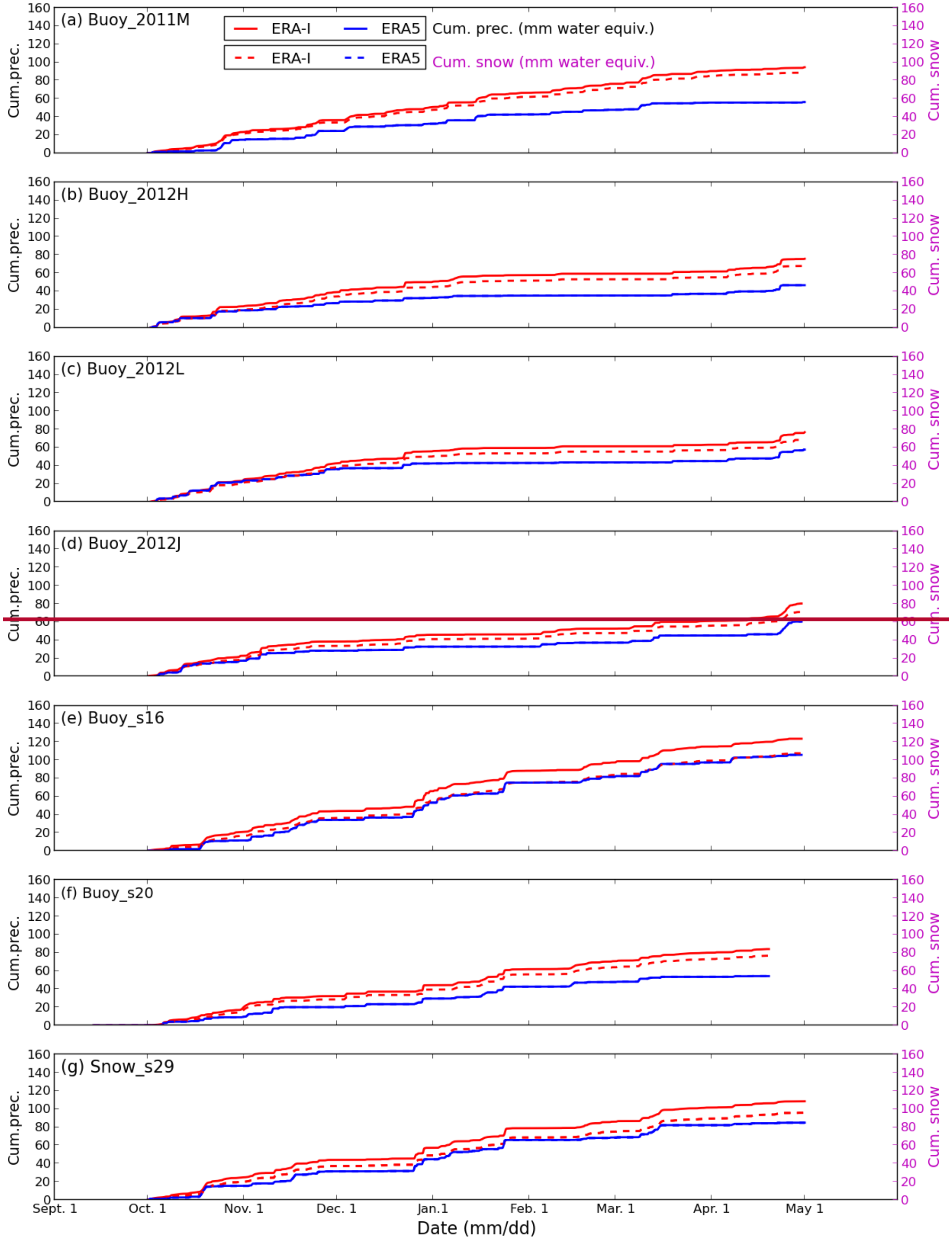

~~**Figure 6. Same as Figure 5, but with accumulation starting from 1 October. The dashed blue lines overlap with the solid blue lines in the panels due to the small differences between the cumulative total precipitation and snowfall in ERA5.**~~

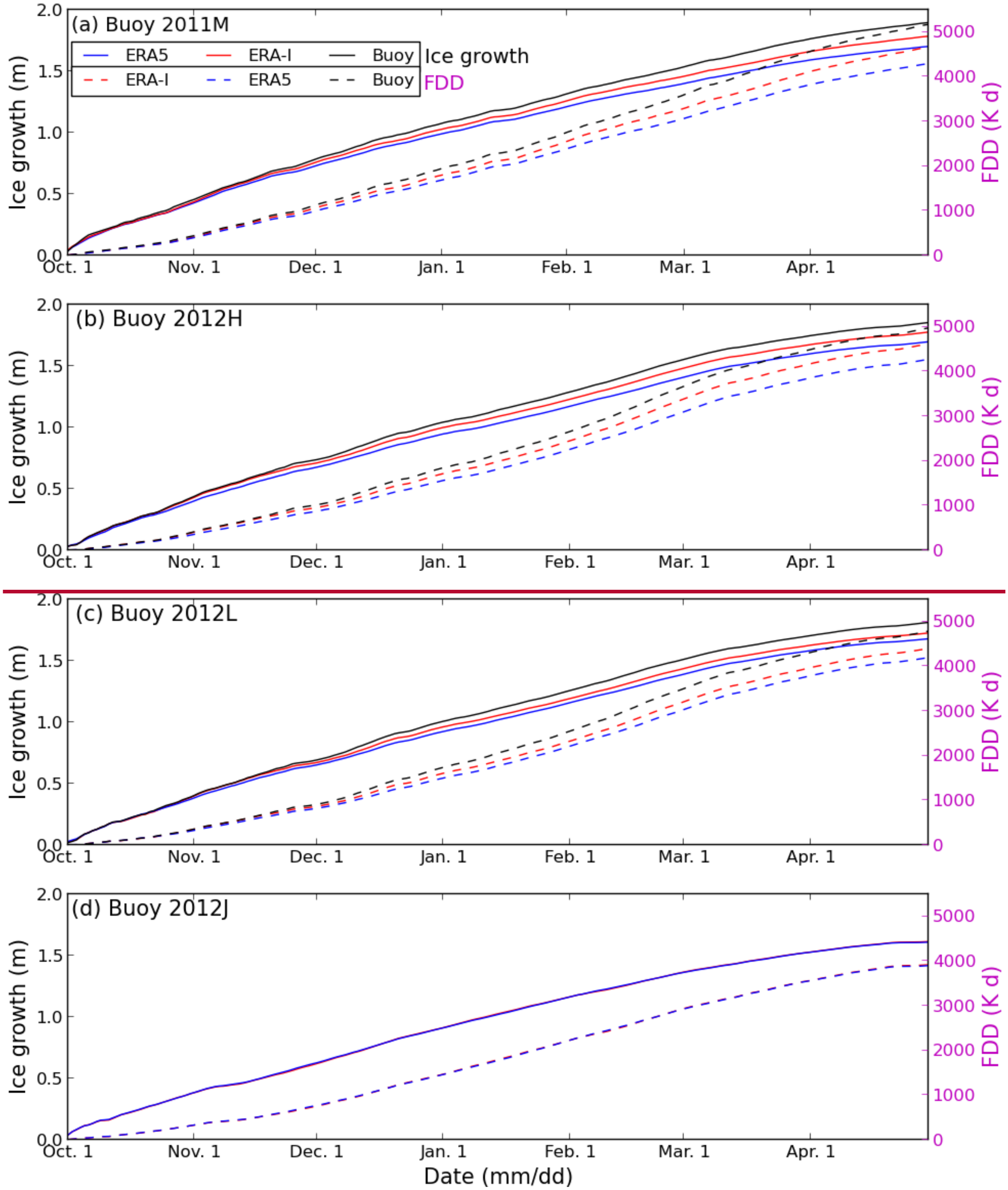

~~**Fig. 7. FDD and estimated ice growth using cumulative FDD based on equation 1 along the trajectories of (a) Buoy 2011M, (b) Buoy 2012H, (c) Buoy 2012L, and (d) Buoy 2012J for freeze-up on 1 Oct.**~~

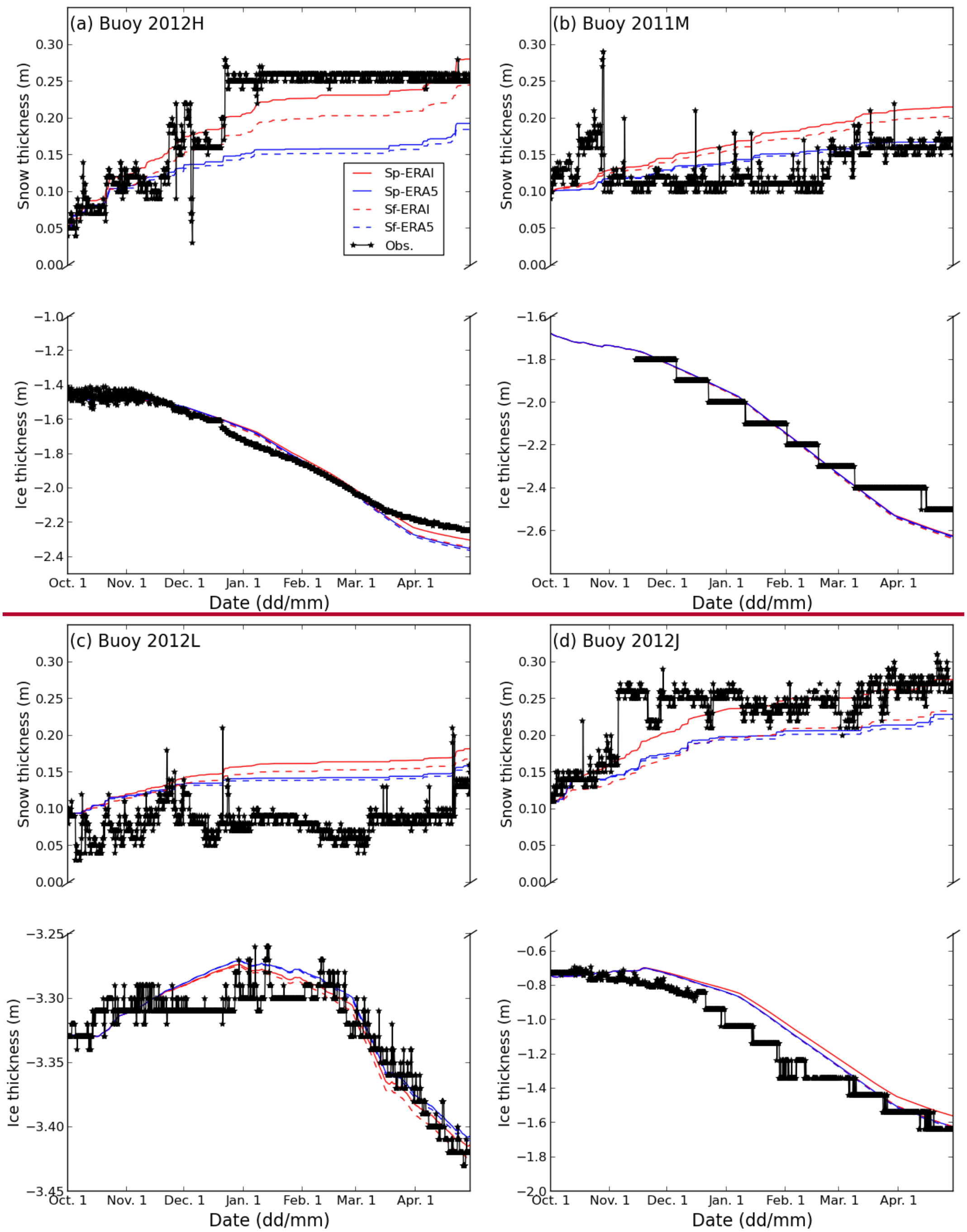
(a) Buoy 2012H
(b) Buoy 2011M
(c) Buoy 2012L
(d) Buoy 2012J
Snow thickness (m)
Ice thickness (m)
Sp-ERAI
Sp-ERA5
Sf-ERAI
Sf-ERA5
Obs.
Oct. 1
Nov. 1
Dec. 1
Jan. 1
Feb. 1
Mar. 1
Apr. 1
Date (dd/mm)

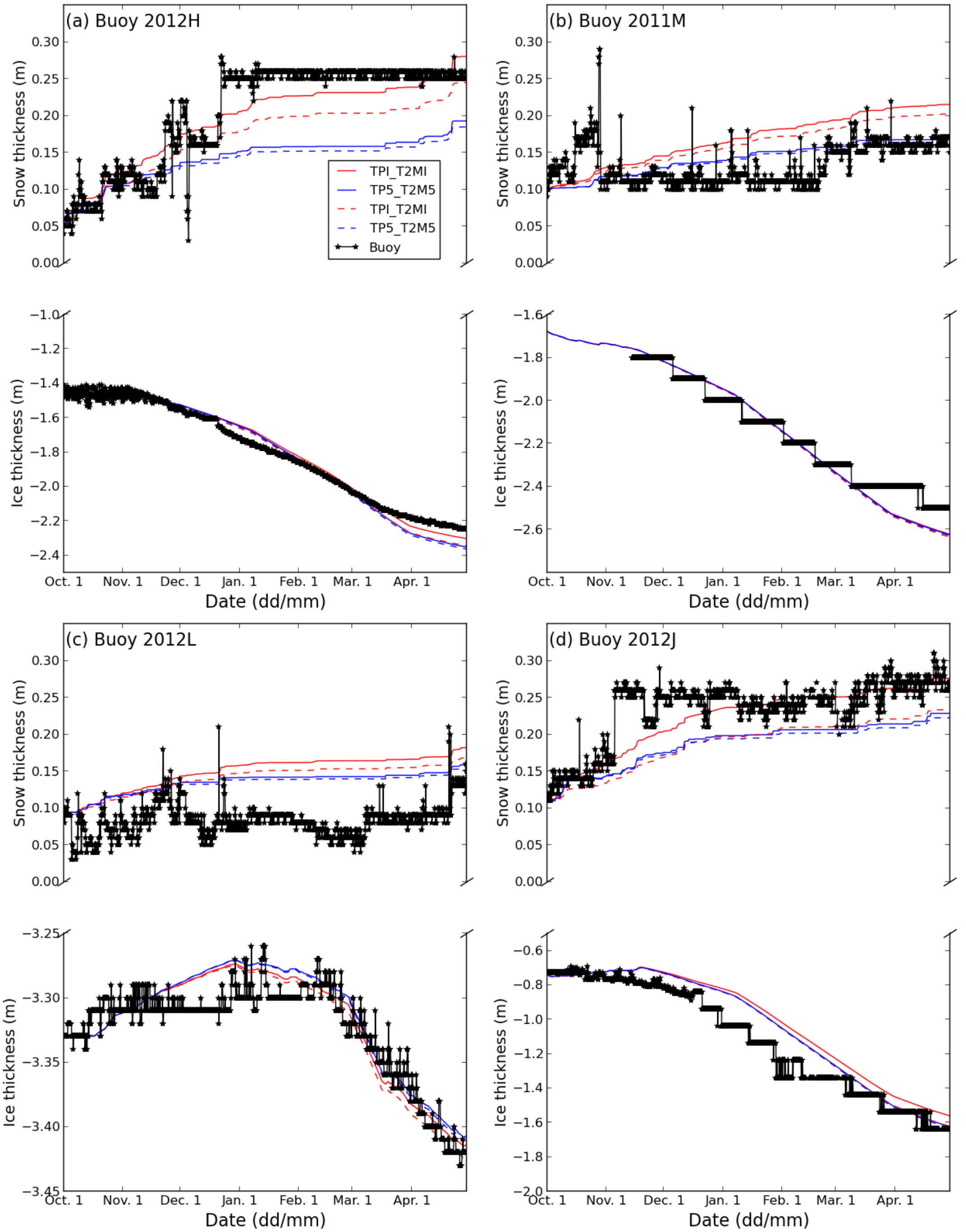

Fig. 8. Evolution of snow and sea ice thickness during freezing season based on simulations with HIGHTSI for (a) b~~B~~uoy 2012H, (b) ~~Buoy~~ buoy 2011M, (c) ~~Buoy~~ buoy 2012L, and (d) ~~Buoy~~ buoy 2012J in the runs of ~~Sp_ERA~~TPI_T2MI, ~~Sp_ERA~~TP5_T2M5, S~~f_ERA~~FI_T2MI, and S~~f_ERA~~F5_T2M5.

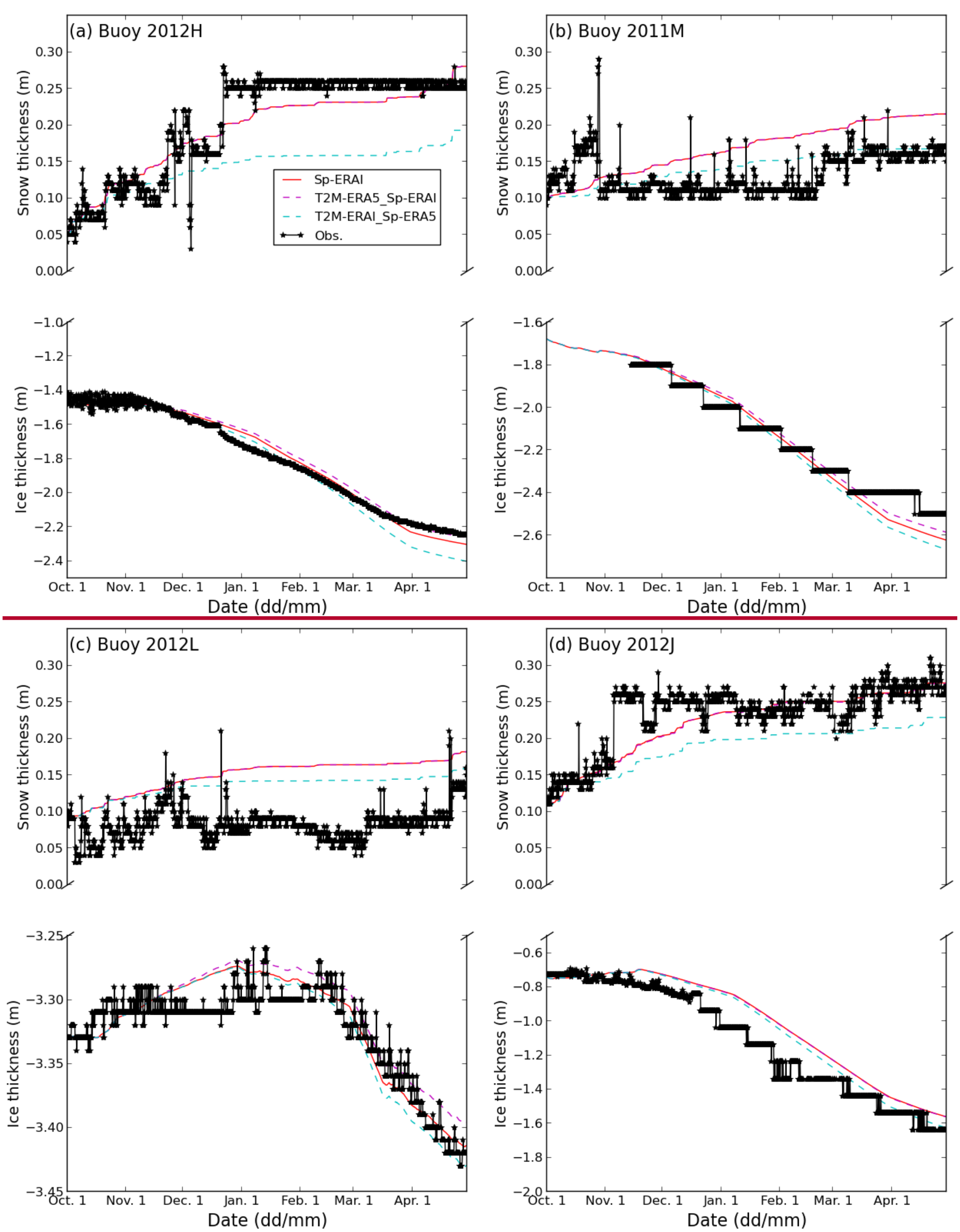

(a) Buoy 2012H
(b) Buoy 2011M
(c) Buoy 2012L
(d) Buoy 2012J
Snow thickness (m)
Ice thickness (m)
Sp-ERAI
T2M-ERA5_Sp-ERAI
T2M-ERAI_Sp-ERA5
Obs.
Oct. 1
Nov. 1
Dec. 1
Jan. 1
Feb. 1
Mar. 1
Apr. 1
Date (dd/mm)

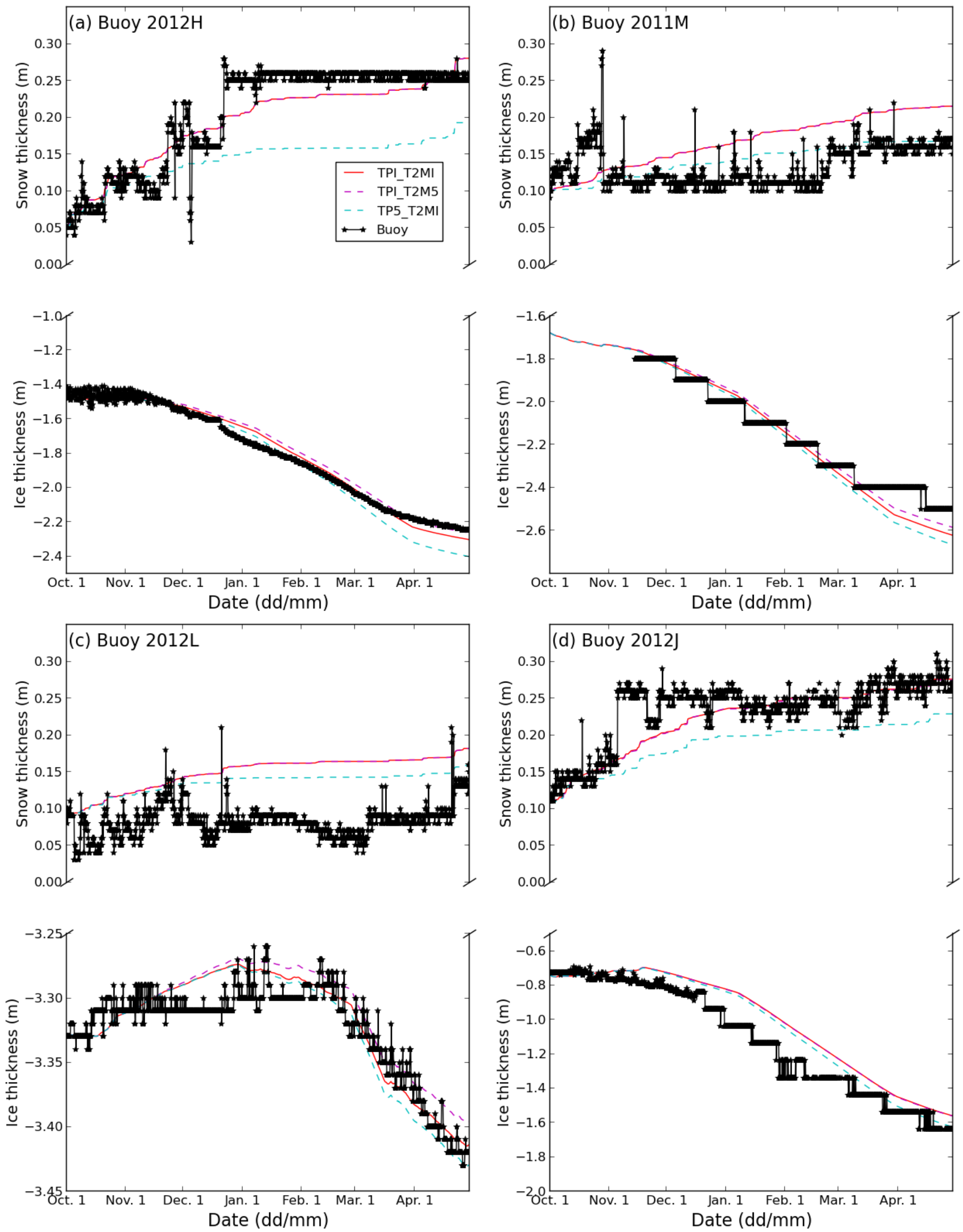

Fig. 9. Same as Fig. 8, but for the runs of ~~T2M-ERA5~~TPI_T2M5, and ~~T2M-ERAI_Sf-ERA5~~TP5_T2MI.